

## On the Penetration of Water into Hot Rock

C. R. B. Lister

' . . . through caverns measureless to man,  
down from a sunless sea,'

Persian Rubaiyat, slightly amended

(Received 1974 August 7)\*

### Summary

This paper develops a theory for the mechanism of penetration of water into hot rock by considering the simplest possible one-dimensional model. The concept of a cracking front is used to separate the convective regime in cracked porous rock from the conductive boundary layer below it. Rock in the boundary layer cools, shrinks and builds up horizontal tensile stress as resistance to creep rises. Cracking occurs when the tensile stress slightly exceeds the overburden pressure and results in the stable downward propagation of a polygonal pattern of sub-vertical cracks. Further cooling shrinkage opens these cracks to the percolation of water so that the effective bulk permeability is a strong function of both crack spacing and temperature. The critical crack spacing is determined by the competing processes of pattern enlargement through stress relief by favoured cracks and the subdivision of columns due to the radial temperature gradients associated with cooling through the cracks themselves. A rudimentary treatment of the transient creep associated with the thermal contraction of virgin rock suggests cracking temperatures between 800 and 1000 °K at depths of several kilometres and a similar treatment of thermally activated crack propagation produces a relationship between front velocity and crack spacing. That permits an approximate solution of the whole problem, resulting in a formula for front velocity

$$u^{2.6} = 7.644 \times 10^{-24} \phi^{0.8} \frac{(T_w - 273)^2 (T_\phi - T_w)^3 (8T_w + T_\phi - 9T_0)^2}{(T_1 - T_w) (T_1 - T_\phi)^{0.8}}$$

where  $\phi$  is a fudge factor and the temperatures are:  $T_w$ —hot hydrothermal,  $T_\phi$ —overburden cancelling creep stress,  $T_0$ —sink,  $T_1$ —original. Maximizing through  $T_w$  permits the calculation of  $u$  and all dependent parameters for any given  $T_\phi$ , itself close to the cracking temperature. If  $T_\phi = 800$  °K, the front velocity is 32 m/yr, the crack spacing is 4.8 cm and the hot hydrothermal temperature is about 462 °K. The power output of the convecting system is about 5 kW m<sup>-2</sup>. Downward propagation of the cracked region seems to be limited by static fatigue failure of the columns under stress, some distance behind the front. The qualitative aspects of the model are in general agreement with ridge crest heat-flow and seismic data, though the sheeted dike complex near the surface of new crust is created by rapid cooling of each new dike by water circulation rather than by a process comparable to the one-dimensional model. Subsequent, deeper, water penetration may occur by processes similar to those described in the model.

\* Received in original form 1973 November 20.

### Contents

This paper covers rather a large field, and it is probably inappropriate for a reader to attempt to go through it from beginning to end at the first confrontation. The sections are listed here in summary form to aid in the selection of those of potential interest, and so that the continuity of the argument in the text need not be compromised. In each case the final result of the section is quoted, whether it be a verbal conclusion or an equation used in further development. Symbols are explained in Appendix I.

*Introduction.* Sets the scene by a brief discussion of geochemical and heat-flow evidence for water penetration at an active ridge crest. Explains the goal and philosophy of the paper.

*The model.* Contains a description of the one-dimensional problem to be considered, and a presentation of the concept of a cracking front on which the solution is based.

*The conductive boundary layer.* Considers the thermal regime ahead of a convection boundary and derives the temperature history of a particle of rock

$$T = T_1 - (T_1 - T_2) \exp\left(\frac{u^2 t}{\kappa}\right). \quad (3)$$

*Contraction and stress.* Develops the stress and strain relations in a material subject to planar thermal contraction. For a high-modulus material like rock, the elastic strain can be neglected at reasonable overburden pressures, and planar strain can be converted into equivalent uniaxial vertical strain

$$\dot{\epsilon} \simeq -2\alpha\dot{T} = \frac{2\alpha u^2}{\kappa} (T_1 - T). \quad (4)(13)$$

*Crack propagation.* This difficult section is at the heart of the theory. It discusses qualitatively, the propagation of a polygonal crack system, and derives an approximate crack edge stress intensity factor

$$k \simeq \frac{1}{2} \frac{n}{1-n} \sigma_c \sqrt{y}. \quad (14)$$

This is compared with the intensity factor found to propagate cracks in single crystal quartz, and an approximate excess uniaxial compressive stress ( $\equiv$  horizontal tension) is obtained

$$\sigma_c \simeq \phi y^{-\frac{1}{2}} (0.03 + 0.0043 \ln u) \text{ kb}. \quad (22)$$

*Crack spacing.* The critical parameter of the crack system is the mean crack spacing, and the phenomenon of *obdivision* is proposed as the controlling factor. A crude estimate of the radial temperature gradient in a propagating polygon is equated with the temperature change needed to produce the excess tensile stress causing the whole system to propagate; whence

$$y \simeq \frac{4\kappa}{u} \sqrt{\frac{T_\theta - T_K}{T_1 - T_K}} \quad (26)$$

The temperature difference  $T_{\phi} - T_K$  is estimated by making use of the qualitative result of the creep analysis, that the creep is in the exponential stress dependence region:

$$T_{\phi} - T_K \approx \phi y^{-1/2} \tag{30}$$

over a fairly wide range of temperatures and creep rates. Combination of these results yields

$$y = \left\{ \frac{16\kappa^2 \phi}{u^2(T_1 - T_K)} \right\}^{0.4} \tag{31}$$

*Permeability.* Calculates the mean permeability of a system of interconnected vertical cracks

$$D = \frac{\sqrt{2}d^3}{12y} \tag{35+}$$

the same for regular hexagonal and square arrays, and finds  $d$  by thermal contraction over  $y$ :

$$D = \frac{\sqrt{2}y^2}{12} [\alpha(T_{\phi} - T_w) - \frac{1}{2}\epsilon_{\phi}]^3. \tag{37}$$

*Convection.* Applies prior results for convection in a porous medium to calculate the total heat flux

$$Q = \frac{D\alpha_w \rho c g (\Delta T)^2}{40\nu_w} = u\rho c(T_1 - T_w) \tag{40}(43)$$

estimates a reasonable lower boundary temperature for convection, and obtains the final formula by combining results from all prior sections

$$u^{2.6} = \frac{\sqrt{2} \times 16^{0.8}}{12 \times 3240} \cdot \frac{\phi^{0.8} \kappa^{1.6} \alpha^3 \alpha_w g}{\nu_w} \cdot \frac{(T_{\phi} - T_w)^3 (8T_w + T_{\phi} - 9T_0)^2}{(T_1 - T_w)(T_1 - T_K)^{0.8}}. \tag{45}$$

The cracking front velocity  $u$  is calculated by maximizing with respect to  $T_w$ , and, choosing various possible cracking temperatures  $T_K \approx T_{\phi}$ , a *table of values* is presented. This *table* may be considered the final result of direct penetration theory.

*Creep.* A discussion of the probable mechanism of *transient* creep at moderate temperature leads to an assertion that the old sinh creep law should apply, and that there should be two quite different activation energies involved. Another *table* compares

$$\sigma = 0.07 \operatorname{arcsinh} \frac{1}{2} \left[ \dot{\epsilon} \exp \left( \frac{80}{RT} - 8.9 \right) \right] + 0.6 \operatorname{arcsinh} \frac{1}{2} \left[ \dot{\epsilon} \exp \left( \frac{40}{RT} - 2.1 \right) \right] \tag{50}$$

to some results of stress versus creep rate and temperature for wet lherzolite, and extends a qualitative fit to somewhat scattered data into the low creep rate regions required by the theory. Further discussion of visco-elastic effects associated with obstructions to dislocation glide yields an estimate of 800 °K for the cracking temperature at about 2 kb overburden pressure. At lower temperatures, cracking could extend much farther into the mantle.

*Creep after chilling.* Finds that creep is negligible during the cooling of the polygonal columns to the water temperature. Further extrapolation of the creep formula derived in the last section estimates the time to half-permeability as

$$\tau \sim 0.002\dot{\epsilon}^{-1} \sim \exp\left(\frac{80}{RT} - \frac{\sigma}{0.07} - 15.1\right) \quad (52)$$

or about  $7 \times 10^{15}$  years at 450 °K and 1.4 kb stress. Any material stiff enough to crack at 800 °K is going to be extremely stiff at 450 °K, and similarly for other cracking temperatures. Continued creep is unlikely to be important in the shutting off of permeability.

*Elastic stability.* A brief discussion of the problem of stability in a mass of quasi-parallel polygonal columns underload. Suggests that incipient instability of the propagating crack system would cause skew stresses and hence an interlocking of the columns.

*Static fatigue.* Considers the problem of how, after demonstrating a decreasing rate of microfracturing, a brittle material fails in compression. The concept of elastic instability offers a solution: continued microfracturing causes subdivision of the material into microcolumns until elastic collapse occurs. The mechanism can operate at depth in a hydrothermal system, and the life has a dependence

$$\langle t \rangle \sim t_0 P^{-1} \exp\left(\frac{H'}{RT}\right) \frac{1}{2} \sinh^{-1}\left(\frac{\sigma}{\sigma'_0}\right) \quad (\text{quartz}) \quad (54)$$

or  $0.1 P^{-1}$  years at 450 °K and 1.4 kb,  $P$  being active water vapour pressure. The diffusion of moisture into the columns is treated by means of the concept of *weakening rate* at varying water pressure. Using the diffusion rate for quartz and a planar diffusion solution approximated to a column gives  $\langle t \rangle \sim 5 \times 10^4$  years at the same stress and temperature as before. The conclusion is that *temperature is the critical parameter*, halving the stress having the same effect as a 16 °K drop in temperature.

*Percolation boundary model.* Develops the concept of static fatigue into a model of how water penetration could be shut off. Volumetric failure of material in the hot upwelling plumes spreads laterally with the migrating hot water into the zone of increased stress around the initial failure. Pulverization of the material reduces the permeability by about  $10^4$  at once, and permits rapid serpentinization to form a completely impermeable layer. Above the layer is a region of cold permeable rock stabilized by the low temperature, and below it the mantle cools slowly by conduction.

*Discussion.* The percolation boundary model is used as a basis for finding a model of ridge crest processes that agrees with data from ophiolite suites, and interpreted heat-flow and seismic results. It suggests that crustal cooling is almost complete within a few kilometres of the spreading axis, and that the Moho boundary is the velocity contrast between slightly serpentinized ultramafic material (velocity 7.4 to 7.8 km s<sup>-1</sup>) and the same material cooled dry.

*Conclusions.* Summarizes many salient points from both theory and discussion, and attempts to use the theory to make a few predictions about hydrothermal conditions near an active spreading centre.

## 1. Introduction

The concept of hydrothermal percolation through the crystalline rocks of the oceanic crust has been invoked by several authors, and it has only awaited confirmation by the collection of suitable evidence. Palmason (1967) has discussed it for the Mid-Atlantic Ridge by comparison with the known geothermal phenomena on Iceland; Talwani, Windisch & Langseth (1971) suggest that it may explain the unexpectedly low heat-flows near the crest and Bodvarsson & Lowell (1972) present a simple model for water flow through contraction cracks. From an entirely different point of view, the analysis of sediments for their heavy metal content, Bostrom & Peterson (1969) have found these metals to be unusually concentrated in pelagic sediments near the East Pacific Rise crest and have invoked hydrothermal elution for their origin. In support of this hypothesis, Bender, Dymond & Heath (1971) have estimated the accumulation rate of Mn along the crest of the ridge to be about 30 times normal and Dasch *et al.* (1971) have found the isotopic ratio of the lead content of crestral material to resemble that of tholeiitic basalt. More recently, Piper (1973) has replotted his own analyses of surface sediment, and those of others, in terms of an inorganic invariant ( $\text{Al}_2\text{O}_3$ ), to obtain sharp concentration peaks for 14 elements near the present-day ridge crest. He has also compared their concentrations in the crestral sediments and in tholeiitic basalt, relative to  $\text{Al}_2\text{O}_3$ , to determine enrichment ratios. These turn out to be reasonable for hydrothermal elution:  $10^2$  for the transition metals except Mn, and about  $3 \times 10^3$  for Mn and other elements such as Pb and As.

This is strong evidence that some percolation occurs, and the next step is to examine the linked questions of how pervasive a phenomenon it may be, how deep it may go and how much it may modify the oceanic crust. Lister (1972) has discussed the implications of detailed heat-flow data and has concluded that the percolation must extend to a depth of several km. This is necessary if the cell pattern is to be effectively forced by surface topography with horizontal wavelengths of that order. Moreover, Ward (1972) has studied the microseismic activity associated with Icelandic geothermal areas and found a concentration of events near a depth of 7 km that would be hard to associate with anything other than the rock cooling process. Thus we know already that the percolation extends to a substantial depth and is caused by the cracking of the brittle crystalline rock upon rapid cooling by the water.

This paper seeks to develop some relationships between the many parameters involved by making a first-order examination of the most likely physical processes. It is organized into sections by physical process, and each section returns as nearly as possible to first principles in order to make the argument self-contained. In some cases, such as the discussion of cracking, a simplified derivation of the fundamental stress relationship is presented even though the result is a special case of more general theory previously published (*cf.* Lachenbruch 1962). The purpose is to make the approximations directly in the physics of the problem where their effect on the answer is absolutely clear. In one other section that deserves special mention, a law of creep has been used that is no longer generally accepted in the field. The problem here is that currently accepted creep laws are empirical devices to fit the experimental data, and no satisfactory data exist for the materials and the conditions expected in the cracking process. To extrapolate such data as do exist by several orders of magnitude via an empirical process would hardly be acceptable, and so a law has been used whose physics, at least, is sound and easily understandable. It may well be applicable to the special case of transient creep in rock materials, even if not to the more widely investigated case of steady-state creep.

Running through the derivation are a series of numerical values that have been chosen by the author as plausible. No realistic accuracies can be specified for any of them because of the unknown nature of the processes involved; it is hoped that the answers obtained are of the right order of magnitude. In later sections, where

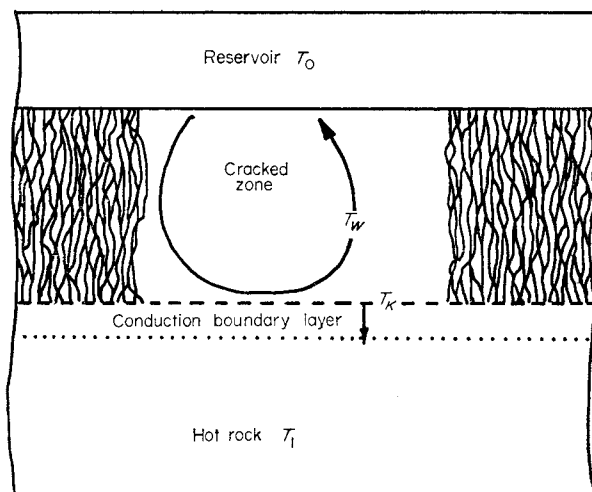


FIG. 1. The one-dimensional cracking-front model. Reservoir  $T_0$  and hot rock  $T_1$  are supplied at time = zero.

competing processes are considered, the numerical results are of some fundamental importance, but there the disparities should be great enough to make the conclusions acceptable to all but the most cynical of readers. It may be well to emphasize that this is a voyage of induction, the application of the most pertinent available physics to a very difficult problem just to see where it will lead. The plan of the approach has had to be changed several times because of the unexpected results obtained, and it is this aspect of the paper that may be of some value.

## 2. The model

To examine the mechanism by which water penetrates hot rock, a geometrically simplified model will be considered. This will allow the development of some quasi-quantitative relationships without introducing geological complications. Suppose that water is penetrating a semi-infinite expanse of hot rock at a planar 'cracking front', it being understood that the cracks are *macrocracks* on a scale of several centimetres and nothing like the 'microfracturing' associated with brittle creep. The situation is detailed diagrammatically in Fig. 1: between the front and the rock surface there is a thermal convective regime maintained by the heat extracted from the hot rock and rejected into the infinite reservoir of cold water above the halfspace. Below the cracking front, there is a thin boundary layer of conductively cooling rock beyond which the rock remains essentially at its original temperature. The actual front is characterized by a temperature at which the rock cracks due to the combination of increasing tensile stress from the cooling shrinkage, and increasing brittleness as its temperature drops. The cracking temperature is a function of many parameters, some of which will be examined in a later section, but if the reader will accept the *concept* of a cracking temperature, the analysis may proceed.

The maintenance of an actual 'front' for the onset of cracking implies that the ability of even incipient water convection to carry away heat is much greater than that of simple conduction. There is no absolutely *a priori* way of showing that this must be the case, considering that the structure of the boundary layer is unknown. However, it will be seen from the analysis that follows that, at least on a large scale, the convective process is orders of magnitude more effective at removing heat than

conduction, so that, on that sort of kilometre scale at least, the front must certainly exist. The details of what may happen at the front are somewhat beyond the scope of a preliminary theory such as this, so that the simplest possible model will be used, and a 'fudge factor' introduced to handle the deviation of the model from reality.

### 3. The conductive boundary layer

Consider first the conductive regime ahead of an advancing front at the cracking temperature, and please refer to Appendix I for a list of the symbols used. The solution for a uniform medium at a constant initial temperature, subject to a moving plane boundary at another constant temperature, is to be found in Carslaw & Jaeger (1959, p. 388); after a settling period, the temperature distribution is

$$T - T_2 = (T_1 - T_2) \left( 1 - \exp \left( - \frac{ux}{\kappa} \right) \right) \quad (1)$$

corresponding to a boundary layer of thickness  $x_0 = \kappa/u$ . The rock may be thought of as 'flowing' toward the boundary with the velocity  $u$ , and as it approaches the front its temperature falls, first slowly and then more rapidly. We can define a time for each particle of rock by putting

$$x = -ut \quad (2)$$

so that  $t = 0$  when  $x = 0$  and  $t \rightarrow -\infty$  as  $x \rightarrow \infty$ . The temperature of the particle can now be expressed as a function of time

$$T = T_1 - (T_1 - T_2) \exp \left( \frac{u^2 t}{\kappa} \right) \quad (3)$$

and

$$\dot{T} = - \frac{u^2}{\kappa} (T_1 - T_2) \exp \left( \frac{u^2 t}{\kappa} \right) = \frac{u^2}{\kappa} (T - T_1) \quad (4)$$

thus quantifying the temperature history of the rock. It may be useful to the reader if we calculate a representative value of the boundary layer thickness for an arbitrary velocity of the same order of magnitude as sea-floor spreading velocities. If  $u = 10 \text{ cm/yr}$ ,  $\kappa = 0.009 \text{ cm}^2 \text{ s}^{-1}$ , then  $x_0 = 270 \text{ m}$ .

### 4. Contraction and stress

A layer of rock in the model consists of an infinite sheet, so that the thermal contraction in all directions in the sheet must either stress the rock elastically, cause permanent creep deformation, or result in cracking. Until cracking occurs, each sheet is undeformed in its own plane (by definition), and may deform in the vertical dimension without affecting its neighbours. Therefore the stress history of each sheet can be considered independently of all the others as long as the material is homogeneous enough on the macroscopic scale of the thermal boundary layer. Since the grain size in ultramafic xenoliths is measured in millimetres, and the thermal boundary layer is metres thick even for front velocities as large as 10 m/yr, this approximation should be valid for the case considered. Thus, the thermal contraction in each layer must be taken up directly as it occurs, and it is possible, in principle, to use stress-strain data to derive the stress history of the layers and determine the cracking temperature at a given overburden pressure. One further implicit assumption will be made: that all strains are small enough not to distort the frame of reference, since accounting for that would cause unnecessary mathematical difficulties.

This subject has been treated at some length by Lachenbruch (1962), who derives a rather general formula for the stress developed in thermally contracting permafrost. His viscoelastic equation covers elastic, Newtonian, Kelvin and Maxwell conditions, as well as power law creep, by suitable assignment of parameters. In the case being considered here, temperature changes of several hundred degrees are certain to be involved, and there are good reasons to suppose that a simple power law of creep will not suffice even over a limited temperature range. Rather than attempt to generalize a complex formula even further, it will be clearer to go back to first principles and derive the simplest possible relationship that leaves the creep law unspecified. Maximum advantage will be taken of the simple geometry being treated, and the rock will be considered to be isotropic as well as uniform. Although this may be unrealistic for hot rock not derived from a stirred magma, it will demonstrate the basic physical relationships, and a more rigorous treatment may always be applied when more is known about the rock material involved.

For the case of planar symmetry, the vertical dimension is free to contract thermally or through creep, and all directions in the plane are identical for an isotropic material. One can then define a 'planar modulus' for a substance that gives its stress response to the elastic part of the deformation. This modulus is connected directly with the Young's modulus by the simple relation

$$M = \frac{Y}{(1-n)} \quad (5)$$

and the overburden pressure, being a vertical compression, results in an equivalent horizontal stress

$$\sigma_H = -M \frac{n\mathcal{P}}{Y} = -\frac{n\mathcal{P}}{(1-n)}. \quad (6)$$

It is this equivalent horizontal compression that must be overcome by the tensile thermal contraction of the rock before cracking can occur, and propagation of the cracks at the necessary rate requires an additional absolute tensile stress in the horizontal direction. Because most creep data refer to uniaxial deviatoric stress, it is probably clearest overall to treat the whole problem as equivalent creep and stress in the vertical direction. The relationship between vertical and horizontal *stress* is defined in (6), so that any additional tensile stress required for crack propagation can be treated as if it were additional overburden pressure. Tensile conditions now begin when the equivalent vertical stress exceeds the overburden pressure directly. *Strain* relations are different from those of stress, because the creep portion of the strain can be presumed to occur without volume change in the rock itself:

$$\dot{\epsilon} = -2\dot{\epsilon}_H, \text{ (plastic)}. \quad (7)$$

The equivalent vertical *elastic* strain follows a different relationship but is of no direct interest. We can thus formulate a stress-strain equation in the horizontal plane and then convert it into its uniaxial vertical equivalent

$$\begin{aligned} \sigma_H &= M \text{ (rate of change of elastic deformation)} \\ &= M \text{ (rate of thermal contraction—rate of creep deformation)} \\ &= M (-\alpha\dot{T} + \dot{\epsilon}_H) \end{aligned} \quad (8)$$

and

$$n\dot{\sigma} = Y(-\alpha\dot{T} - \frac{1}{2}\dot{\epsilon}) \quad (9)$$

that now relates directly to uniaxial creep data.



It is tempting to incorporate a simple creep law of the type

$$\dot{\epsilon} = f(\sigma, T)e^{-H/RT}$$

into the above equation and solve, but it must be remembered that the creep we are dealing with here is *transient* creep, not a steady-state creep as defined by the equation. At a given strain rate, the stress developed rises with increasing strain, or, alternatively at a given stress, the creep rate decreases gradually toward its steady-state value. It is more appropriate to consider some rough orders of magnitude, using the available circumstantial evidence to guess at what may occur, and return to a fuller consideration of creep after discussing the convective thermal transfer regime.

The initial rock temperature, a typical hydrothermal temperature, and the expansion coefficient of ultramafic rock are all quite well known, so that the maximum feasible equivalent uniaxial plastic strain can be calculated readily

$$\epsilon_{\sigma=0} = 2\alpha(T_1 - T_w) \simeq 3\% \quad \text{for } T_w = 500^\circ\text{K} \quad (10)$$

and, using the known modulus and Poisson's ratio for such rock, a maximum conceivable equivalent uniaxial stress for the completely elastic case

$$\sigma_{e=0} \simeq (Y/n)\alpha(T_1 - T_w) = 64 \text{ kb.} \quad (11)$$

This can be compared with the overburden pressure due to 1 km of rock

$$\mathcal{P} = gh(\rho - \rho_w) \simeq 0.2 \text{ kb km}^{-1}, \quad (12)$$

and it is clear that a considerable amount of creeping must take place if the penetration is to be limited to the micro-earthquake depth of 7 km (Ward 1972). In fact, if the maximum stress is indeed of the order of 2 kb or less, then the elastic strain represents a negligible portion of the total strain, and one may be able to write

$$\dot{\epsilon} \simeq -2\alpha\dot{T} = \frac{2\alpha u^2}{\kappa} (T_1 - T). \quad (4)(13)$$

This demonstrates that the strain rate rises steadily as the temperature decreases from the initial temperature. The resistance to creep should increase as the temperature decreases, and therefore the stress may build up quite rapidly as the cracking temperature is approached.

## 5. Crack propagation

As soon as the rock cracks, it should be chilled rapidly by the percolating water, and, since the stress now remains steady at the overburden pressure, the creep rate should drop sharply. (The question of static fatigue and failure will be treated later.) To an approximation then, the width of the cracks that open depends mainly on the drop in temperature between the cracking temperature and the temperature of the percolating water, and also on the crack separation. Whether the cracking assumes the random orthogonal pattern often observed in fractured permafrost (Lachenbruch, 1962) and in drying mud (Corte & Higashi 1960) or the more regular quasi-hexagonal pattern sometimes found in cooled igneous rock (Beard 1960) some estimate of the average crack separation must be made. It will be shown later that the pattern of the cracking has little effect on the bulk permeability of the cracked rock, but the mean separation is a critical parameter. In this section we shall examine the mechanics of the cracking process and derive an estimate of the excess tensile stress needed for crack propagation.

The problem of brittle fracture into a semi-infinite medium stressed at its surface has been treated extensively by Lachenbruch (1961, 1962). The case we have to

consider differs from his in several ways, however, in that the cracking front is not near a free boundary, the cooling is due entirely to circulation through the cracks themselves, and, most importantly, we are interested in stable propagating solutions rather than essentially static ones. Lachenbruch (1962) treats his fracturing as if it were primarily the well-known catastrophic brittle type, but although the permafrost does occasionally crack with a loud report, the final depth of the fractures is probably determined by stable crack propagation under conditions of decreasing stress concentration at the crack tip. He incorporates this by assigning a limiting 'crack edge stress intensity factor' (Irwin 1958) for the termination of propagation that is less than the value needed to cause catastrophic crack acceleration. According to the theory of macroscopic fracture of Irwin (1958), crack or flaw extension occurs by a plastic deformation process at tip stress concentrations too low to cause failure. Whether or not plastic deformation is really involved in the fracturing of crystalline materials, Martin (1972) has shown that the stable propagation of cracks in single-crystal quartz obeys a reasonable law of variation against temperature, water vapour pressure and stress. The similarity of this law to those for plastic deformation is more than coincidental, since the plasticity of crystalline materials is due to dislocation movement and grain recrystallization, and a crack can be considered as an extreme case of dislocation climb. The important conclusion is that crack growth continues at a finite rate for any finite value of tensile stress concentration at the tip, at least for glasses and single crystal materials where the crack cannot be terminated at a grain boundary. We shall assume that the rock at the cracking front, although fine-grained and multi-mineralic, is brittle enough at the cracking temperature for the grain-boundary termination mechanism not to be effective at the actual applied stress and rate of crack advance. It is possible that the application of Martin's (1972) result to crack propagation in a mafic rock underestimates the medium temperature strength. In addition to a different intrinsic propagation rate, it is probable that the activation energy, and hence the variation of strength with temperature, is also different from that in quartz.

Lachenbruch (1961) presents the variation of crack edge stress intensity factor with crack depth for a single infinitely long crack in either an infinite or semi-infinite medium. Two stress systems are considered: a finite region of constant tensile stress near the reference plane, and the case of steadily increasing stress away from that plane, corresponding to the lithostatic head. Near a hydrothermal cracking front, the lithostatic pressure can be considered constant through the thin thermally stressed layer, but the excess tensile stress due to thermal contraction passes through a maximum near the cracking front (see the sketch in Fig. 2). Behind the front, excess stress is relieved by elastic contraction of the columns isolated by the cracks, and ahead of the front, the thermal gradient ensures a steady decrease in total contraction and therefore in the total tensile stress. The system is elastically stable, because any tendency for the cracks to propagate ahead of the thermal front causes the stress field behind the front to decay in the same distance from a lower peak stress. A simple qualitative argument will show that the stress ahead of a crack has little effect on the stress concentration at its tip.

It is well known (Irwin 1958) that the crack edge stress intensity factor of a crack in uniformly stressed material is proportional to the square root of crack length. Consider a hypothetical case where a crack pre-existing in unstressed material just penetrates into a stressed region: the unstressed region contributes nothing to stress concentration at the crack tip, and, if the penetration into the stressed region is infinitely small, so is the stress concentration. Hence, only the stress behind the cracking front contributes to its propagation, and, if the stress relief in the columns were purely elastic, it would be possible in principle to calculate the crack edge stress intensity factor for any given polygonal system. Since the non-uniform thermal gradients and the partial plasticity of the material invalidate any careful calculation

of the elastic strain relief, a simple qualitative argument will be used to estimate the order of magnitude of the stress concentration. In the elastic case, the tensile stress decrease behind the front can be approximated by a linear stress decrease of a length comparable to the diameter of the columns, and probably about half. The problem of non-planar isotherms can be handled, at least for the calculation of excess tensile stress, by the introduction of a numerical factor of deviation from the idealized planar model. Since the column centres are not fully cooled in the real situation, the equivalent excess tensile stress of the idealized model must be increased. The factor is therefore greater than unity, and will be lumped with the material fudge factor in the following discussion.

The solutions presented by Lachenbruch (1961) were obtained by two-dimensional transform methods (Muskelishvili 1953) applicable only to infinite cracks. However, if we can assume that the interaction effect of the polygonal geometry is fully accounted for by the quasi-linear stress relief behind the front, the results can be applied qualitatively to crack tip regions away from the polygonal corners. The useful case is one of uniform stress increase toward the crack tip, but tension rather than the lithostatic compression considered by Lachenbruch (1961). The crack edge stress intensity factor is given by the product of the peak stress, the square root of the stressed length, and a numerical factor that is 0.636 for the symmetrical infinite-body case and about 0.68 for a halfspace with free surface. The case of the stress-relieved columns is somewhere between those quoted, and, to an accuracy that is quite sufficient considering the nature of the assumptions, may be taken as embodying a numerical factor of about 2/3.

To recapitulate the model as derived so far, it is suggested that the crack edge stress intensity factor in a propagating polygonal system is of the order of:

$$k \simeq \frac{1}{3} \frac{n}{1-n} \sigma_c \sqrt{y} \quad (14)$$

with a possible further correction for non-planar isotherms, and where the horizontal tension has been referred to the equivalent vertical uniaxial stress. The situation has been sketched in Fig. 2, where two cracks out of a polygonal propagating series are shown in section. The gradual opening of the cracks behind the tip is a consequence of the elastic relaxation we have discussed, plus some additional cooling shrinkage. It is important in generating the picture because, since the crack flow resistance varies as  $d^{-3}$ , the circulation does not extend efficiently to the crack tips, and it is permissible for isotherms to intersect the crack wall. This in turn prevents the columns from having large radial temperature gradients near the crack tips and a tendency to subdivide because of circumferential tension.

It is now appropriate to try to compare the crack edge stress intensity factor derived above for a propagating polygonal system with that in the experiments described by Martin (1972). His prismatic blocks of quartz had 3.2-mm diameter holes in the centre of faces about 32 × 20 mm. They were cracked by applying compression along the major dimension, and the crack propagation velocities were measured when the (two) cracks extended about 2.8 mm from the hole parallel to the applied compressive stress. The geometry does not lend itself to easy estimation of the crack edge stress intensity factor, since the presence of the cracks grossly distorts the stress field around the circular hole, and there is a tendency for cracks to propagate along the major compression direction even in the absence of a hole. A very crude estimate can be made by applying the results of Lachenbruch (1961, Table 6), for the edge stress intensity factor of an infinite crack extending beyond a planar stressed layer, to the known stress distribution around a small circular hole (Timoshenko & Goodier 1970, p. 90). The thickness of the equivalent uniformly stressed layer will be taken as the half-peak decay distance of the stress around the hole, about 0.14 of

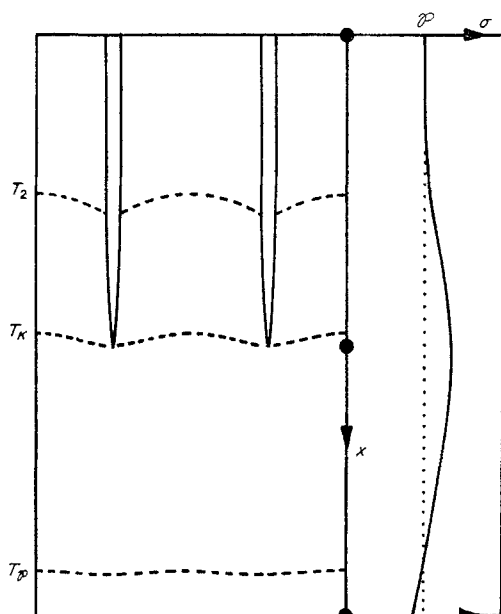


FIG. 2. Possible temperature and stress distribution near the cracking front. Two cracks out of a parallel propagating series are shown. Isotherms are qualitatively sketched in only, and the stress graph is meant to represent a mean stress within the structure rather than that along any particular section line. The conductive boundary layer extends well beyond the lower end of the diagram.

the hole radius, and the stress as the peak stress, equal to the applied stress. The correction factor from Lachenbruch (1961, Table 6) is therefore about 0.05 and the crack edge stress intensity factor for the Martin (1972) experiment can be written

$$k_m \simeq 0.026 \sigma_m \quad \text{kb cm}^{\frac{1}{2}}. \quad (15)$$

Equations (14) and (15) can be combined to give the excess equivalent vertical compression needed to propagate the polygonal crack system

$$\sigma_c = 0.08 \phi \frac{1-n}{ny^{\frac{1}{2}}} \sigma_m, \quad (16)$$

where the 'fudge factor'  $\phi$  represents a combined correction for non-planar isotherms in the polygonal system (perhaps of the order of  $\times 2$ ) and the difference in the cracking behaviour between quartz and a mafic rock.

The formula that Martin (1972) derived for the time required by the cracks to advance a given distance is

$$\frac{t_1}{t_2} = \left( \frac{P_1}{P_2} \right)^{-0.95} \exp \frac{25.8}{R} \left( \frac{1}{T_1} - \frac{1}{T_2} \right) \exp \left( \frac{\sigma_2 - \sigma_1}{0.027} \right). \quad (17)$$

Using his result that a crack advances at  $7 \times 10^{-6} \text{ cm s}^{-1}$  for  $T = 514^\circ \text{K}$ ,  $\sigma = 0.525 \text{ kb}$ ,  $P = 0.405 \text{ bars}$ , converting to velocities and replacing the stress exponential by  $(2 \sinh)$  so that zero stress causes zero velocity of propagation, we have

$$u = \exp(-5) P \exp \left( - \frac{25.8}{RT} \right) 2 \sinh \left( \frac{\sigma_m}{0.027} \right) \text{ cm s}^{-1}. \quad (18)$$

The experimental geometry stress  $\sigma_m$  needed to cause the cracks to propagate at various rates can now be estimated, and for  $u = 10, 100, 1000$  cm/yr,  $P = 1$  kb, and  $T = 600^\circ\text{K}$ ,

$$\sigma_m = 0.12, 0.18 \text{ and } 0.24 \text{ kb.} \quad (19)$$

The equation is clearly in the exponential region of the sinh term, and remains so for temperatures up to  $800^\circ\text{K}$ , so that the correct expression for  $\sigma_c$ :

$$\sigma_c = 0.0022\phi \frac{1-n}{ny^{\frac{1}{2}}} \operatorname{arcsinh} \left( \frac{u}{2P} \exp \left( 5 + \frac{25.8}{RT} \right) \right) \quad (20)$$

can be replaced by the simpler approximate relation

$$\sigma_c = 0.0022\phi \frac{1-n}{ny^{\frac{1}{2}}} \left( \ln \frac{u}{P} + 5 + \frac{25.8}{RT} \right) \quad (21)$$

for  $u \geq 1$  m/yr and  $T \leq 800^\circ\text{K}$ . For the chosen plausible values, this becomes

$$\sigma_c \simeq \phi y^{-\frac{1}{2}} (0.03 + 0.0043 \ln u) \text{ kb} \quad (22)$$

with  $u$  now in m/yr. Therefore, provided only that  $\phi$  be numerically not too large, and  $y$  not too small, the excess tensile stress required to propagate the main polygonal system is small and essentially negligible compared to the overburden pressure at depths of several kilometres. This means that the crack propagation process has little effect on the cracking temperature at a given velocity of front propagation, but it still controls the front velocity by modulating the crack spacing. In fact, for the planar model to be applicable at all, a mechanism must operate to keep the crack spacing small compared to the thickness of the thermal boundary layer.

## 6. Crack spacing

When cracks propagate from a surface shrunk by cooling or desiccation, they relieve tensile stresses over horizontal distances comparable to their depth (Lachenbruch 1961). As cooling or drying penetrates deeper than the initial crack spacing, the polygonal pattern becomes unstable, and certain cracks are favoured while others become inactive. The size of the active polygonal system tends to increase with time, remaining comparable to the thickness of the shrunk layer: an extreme example of this has been reported by Willden & Mabey (1961). If the oceanic crust cracked in this way, a few isolated cracks would form at kilometre spacing, as suggested by Bodvarsson & Lowell (1972).

The important counter-example is the manner of columnar cracking frequently found in cooled lava: columns of a constant size extend all the way through a flow even when the depth of that is many times the diameter of the columns. Lachenbruch (1961) has suggested that the spacing is set initially by the thickness of the cooled layer when cracking begins, and is then maintained because rock plasticity at high temperatures stabilises the crack pattern. A similar argument should apply to drying mud, however, since it is plastic prior to desiccation. Perhaps the most telling example in support of an independent control of the crack spacing is the rare occurrence of lava flows with approximately semi-circular cross-section that exhibit columnar jointing. The columns are not pie-shaped, but remain of roughly constant diameter all the way into the centre of the flow, even though they converge from all directions. In this case, the mechanism that prevents widely-spaced cracks from being favoured fails when the crack spacing becomes too small, and the pattern changes to reduce the number of columns.

The great difference in cracking behaviour between drying mud and columnar lava flows can be resolved at once if the cooling of the lava occurs through the polygonal cracks themselves, but the drying of the mud is primarily a phenomenon of bulk diffusion. In the latter case, the polygonal pattern has no influence on the thickness of the contracted layer or its rate of extension, and therefore itself conforms to the scale imposed by diffusion. If the cooling occurs through the cracks themselves, however, the polygonal pattern has a direct effect on the process, and the situation lends itself to a stable propagating solution because of the properties of permeable convecting systems (as will be discussed in a separate section). The basis of the size-stabilizing mechanism is also fairly obvious: if the columns try to become too large, radial temperature gradients within them cause sufficient hoop tension to induce subdivision. That this actually occurs in nature is confirmed by examination of Plate 2, Fig. 1 in Lachenbruch (1962): in a largely regular hexagonal pattern of separated columns, there are some orthogonal junctions suggestive of subsequent cracking. They subdivide polygons with non-orthogonal corners that were larger than the stable set.

A brief digression may be in order to make this argument clear to readers who have not perused the text accompanying the figure cited from Lachenbruch (1962). An isolated straight crack relieves the perpendicular tension near it almost completely, but has only a small effect on the parallel tension. Therefore, if subsequently another crack approaches the first one, they will join orthogonally; or, if a subsidiary crack propagates out of the first one, it will do so orthogonally to relieve the principal residual stress. There is little alternative but to explain *non-orthogonal* corners ( $\approx 120^\circ$ ) as being formed by simultaneous propagation of all three cracks perpendicular to the plane of observation. Lachenbruch (1962) attempts to deal with the problem by suggesting that cracks propagating laterally under violent supercritical conditions would tend to fork at about  $120^\circ$  angles, but there is no reason to suppose that such violent cracking occurs during the cooling of a lava flow, and considerable difficulty in envisaging how it could produce a regular pattern. Such a pattern is, however, entirely consistent with a cracking front model, and the consistency with which non-orthogonal joints occur in columnar lavas provides additional support for the concept.

To say that radial temperature gradients stabilize the size of a propagating polygonal crack system is easy; quantifying the idea is another matter. The example of polygon splitting already referred to (Lachenbruch 1962) is the crudest way in which the pattern may be subdivided. The time and place of such a subdividing crack is dependent upon the distribution and size of flaws in the material, since a crack cannot start spontaneously. It is possible that subdivision is not an easy or predictable process during crack propagation, but as long as it can occur sooner or later, one can argue that the important process is *obdivision*. Cracking muds and permafrost layers tend to favour the gradual development of larger patterns as the cracks deepen, and, if we may coin the term 'obdivision' for this process, it is the stabilization against obdivision that is important. Fig. 3 depicts one of a number of ways in which a regular hexagonal pattern may obdivide, and the possibilities in the somewhat irregular pattern (such as Lachenbruch 1962, Pl. 2, Fig. 2) are more complex still. However, in any pattern containing a predominance of three-plane joints, it is the failure of some of these 'corner triplets' to propagate with the cracking front that causes obdivision.

Should a corner triplet of cracks fall behind the main cracking front, it comes into the region of geometric stress relief of the cracks further ahead. In the absence of thermal gradients induced by those cracks, it would see a lower peak excess tensile stress and just as rapid a decay of that stress behind the crack tip, so that its propagation rate would slow and the triplet would be quenched eventually. Acting against this reduction of crack tip stress intensity factor is the hoop stress induced in the

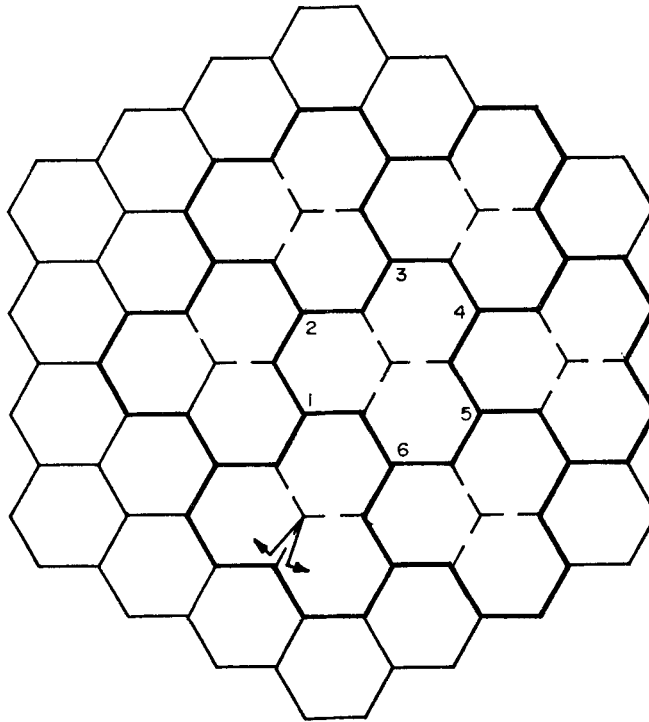


FIG. 3. Diagram of one possible *obdvision* process whereby a regular hexagonal pattern could be enlarged by a factor of  $\sqrt{3}$  in linear size. The small arrows indicate the action of hoop stress aiding the propagation of a lagging triple corner. The polygons remaining do not look like hexagons, but each is still joined to its neighbours by six triple corners. A less regular initial pattern could obdvide by a smaller scale factor into a pattern of similar irregularity.

larger column by the radial temperature gradient, as indicated by the arrows in Fig. 3. In principle one could calculate how much radial temperature difference is needed in a normal column of the pattern for the corner triplet to be accelerated if it falls behind inside the larger, incipiently obdvided column. We are interested here in an order-of-magnitude estimate, and not in an attempt to solve a complex three-dimensional problem with intersecting cracks. Crude estimate though it is, the simplest approach is to assume that the normal radial temperature difference in a column should be comparable to the temperature difference required to generate the excess tensile stress that causes the cracking front to propagate. There is still a potential geometric problem in the heat-flow, since the region of interest is right at the crack tips, at the transition from crack-cooling to planar conduction cooling. The easiest way to handle this without becoming involved with the complexities of water flow near crack tips is to make another oversimplifying assumption, wrong in detail but correct in order of magnitude. Let us calculate the radial temperature difference in a cylinder steadily cooled from the outside at a rate equal to the product of the front velocity and the vertical temperature gradient near the cracking front. The calculation neglects longitudinal transport of heat, but it does accurately reflect the radial gradient that *would* be observed some distance behind the cracking front *if* the vertical temperature gradient were continued by the right amount of cooling. The longitudinal temperature gradient in the cylinder would become constant again, and so would

contribute nothing to the heat balance of the cylinder interior. For the steady cooling case

$$\dot{T} \pi r^2 = 2\pi r \kappa \frac{dT}{dr} \quad (23)$$

and

$$\Delta T_r = \int_0^{y/2} \frac{dT}{dr} = \frac{\dot{T} y^2}{16\kappa}. \quad (24)$$

Now, substituting for  $\dot{T}$  from (4) at  $T_K$ :

$$\Delta T_r = \frac{u^2 y^2}{16\kappa^2} (T_1 - T_K) \quad (25)$$

and, using the assumption that  $T_\phi - T_K \simeq \Delta T_r$ , we can write

$$y \simeq \frac{4\kappa}{u} \sqrt{\frac{T_\phi - T_K}{T_1 - T_K}}. \quad (26)$$

A proper evaluation even of this crudely approximate relation should utilize a full creep equation as well as the value of  $\sigma_c$  obtained from (20) or (21). The creep problem is so especially difficult that it is better to leave it to a subsequent discussion and merely note that, over a small temperature range

$$T_\phi - T_K = \sigma_c \left( \frac{d\sigma}{dT} \right)_\dot{\epsilon}^{-1} \quad (27)$$

where  $\dot{\epsilon}$  is the creep rate near the cracking front, a function of expansion coefficient and rate of temperature change. A representative value is  $2.8 \times 10^{-8} \text{ s}^{-1}$  for  $u = 34 \text{ m/yr}$ , and reference ahead to Table 2 will demonstrate the significance of (27). In the region where creep rate is an exponential function of stress, the stress at a given creep rate is a function of inverse temperature, so that

$$\left( \frac{d\sigma}{dT} \right)_\dot{\epsilon}$$

is not a strong function of temperature or strain rate: for example

$$\left( \frac{d\sigma}{dT} \right)_\dot{\epsilon} = 0.036 \text{ kb/}^\circ\text{K @ } T = 650^\circ\text{K}, \quad 2.8 \times 10^{-10} < \dot{\epsilon} < 2.8 \times 10^{-4} \quad (28a)$$

$$0.026 \text{ kb/}^\circ\text{K @ } T = 750^\circ\text{K}, \quad 2.8 \times 10^{-9} < \dot{\epsilon} < 2.8 \times 10^{-4} \quad (28b)$$

$$0.020 \text{ kb/}^\circ\text{K @ } T = 850^\circ\text{K}, \quad 2.8 \times 10^{-8} < \dot{\epsilon} < 2.8 \times 10^{-6} \quad (28c)$$

$$0.007 \text{ kb/}^\circ\text{K @ } T = 850^\circ\text{K}, \quad \dot{\epsilon} = 2.8 \times 10^{-9} \quad (28d)$$

Equation (21) demonstrates that  $\sigma_c$  is also not a strong function of  $u$  or  $T$  in this range, and the corresponding values are

$$\sigma_c = 0.036\phi y^{-\frac{1}{2}} \text{ @ } T = 650^\circ\text{K}, \quad u = 34 \text{ m/yr} \quad (29a)$$

$$\sigma_c = 0.025\phi y^{-\frac{1}{2}} \text{ @ } T = 750^\circ\text{K}, \quad u = 34 \text{ m/yr} \quad (29b)$$

$$\sigma_c = 0.017\phi y^{-\frac{1}{2}} \text{ @ } T = 850^\circ\text{K}, \quad u = 34 \text{ m/yr} \quad (29c)$$

$$\sigma_c = 0.0074\phi y^{-\frac{1}{2}} \text{ @ } T = 850^\circ\text{K}, \quad u = 3.4 \text{ m/yr} \quad (29d)$$



with the *RHS* coefficient generally showing a gradient of 0.009 per decade of change in  $u$ . Combinations of the (a, b, c, d) equations yields

$$T_{\phi} - T_K \simeq \phi y^{-1/3} \text{°K} \quad (30)$$

over the range of equation (29) and, finally, we can write

$$y \simeq \left( \frac{16\kappa^2 \phi}{u^2(T_1 - T_K)} \right)^{0.4} \quad (31)$$

with a good measure of applicability over a wide range of conditions and a low-power dependence on the fudge factor  $\phi$ .

Since the subject of columnar jointing in lava flows has been brought up, a brief digression to it seems necessary here. The overburden pressure is negligible during the cooling of a surficial lava flow, and the convenience of having the creep-induced stress in the logarithmic region (referred to inverse temperature and creep rate) is no longer available. The cracking temperature could be considerably higher than 850 °K, and a serious problem arises with the extrapolation of Martin's (1972) results to such high temperatures. It is already marginally permissible to extrapolate results for quartz between 300 and 500 °K to mafic rock at 650–850 °K, and it can be justified only by the relative insensitivity of the result (31) to the fudge factor involved. The higher the temperature, the more sensitive the result is to an error in the heat of activation for crack propagation, especially because of the similarity in form between (20) and (50). Unless the lava is dry enough to have a different activation energy for internal creep from that associated with water-filled cracks, the equations become so similar that whether or not a cracking front may propagate depends on the velocity  $u$  that can be maintained, and its effect on (50) through  $\dot{\epsilon}$  (given by 13). If the water in the cracks does lower the activation energy relative to that in the bulk rock, then the slower variation of  $\sigma_c$  with temperature will set a value of  $T_K$  that is relatively insensitive to  $u$ , as it is in the overburden-stressed case. Much has been made (cf. Lachenbruch 1961) of the supposed resistance of plastic materials to cracking, but the author's own experience with hot or partially cured epoxy resins bears out the general conclusions of Martin (1972). A crack is an extreme form of dislocation climb, and therefore moves more easily through a weak material than in a cold and strong one, just as do the creep dislocations. The principal difference is that all the stresses become small, and it is easy to apply enough positive hydrostatic pressure to prevent tensile conditions from developing. The conclusion on columnar lavas has to be that cracking is readily possible, but may have a threshold front velocity associated with it. The polygon size to velocity relationship may remain similar to (31), but better high temperature data are needed to define even that crude estimate.

## 7. Permeability

A solid medium penetrated by a system of interconnected cracks can be considered to have a uniform bulk permeability on a scale substantially larger than the mean crack spacing. The permeability is an important parameter because the thermal convective transport of heat from the cracking front determines its rate of advance, the heat liberated by the cooling rock being carried away by the percolating water. Since the crack spacing is unlikely to be greater than a few metres, and the penetration depths seem to be in the kilometre range, a consideration of the convective problem can treat the permeability as bulk. This is the same approach as that used by Harlow & Pracht (1972), but, instead of applying a formula of doubtful validity in the special model we are considering, the relationship between crack spacing and permeability will be examined directly from first principles. We shall make use of the expected

predominance of vertical cracks in the planar model by confining the discussion to arrays of vertical cracks.

Bulk permeability is defined by Darcy's Law

$$\rho v = - \frac{D}{\nu} \nabla P \quad (32)$$

where  $D$  is scalar for an isotropic medium but may be a tensor in the general case. Now, it can be calculated readily that the flow through a plane crack is given by

$$v = - \frac{1}{12} \frac{d^3}{\eta} \nabla P \cos \phi \quad (33)$$

where  $\phi$  is the angle between  $\nabla P$  and the crack plane. Multiplying through by  $\rho$  and comparison with Darcy's Law gives, in the pressure gradient direction

$$D = \frac{1}{12} \frac{d^3}{y} \cos \phi \quad (34)$$

for any system of plane parallel cracks separated by spacing  $y$ . Now the cracks caused by hydrothermal penetration into a real rock are neither plane nor parallel sided. The latter is unlikely to be much of a problem because the flow is laminar and the roughness of the crack walls becomes important only if there are gross variations in crack width on a scale of a few widths. Casual observation of cracks and jointing in rock exposures suggests that they are fairly smooth on this scale, and that the flow will not be much less than in the smooth planar case. This will now be assumed, and the problem of the randomized crack pattern will be treated in a simple way.

A real quasi-random pattern is observed in Lachenbruch (1962, p. 12, Fig. 2), and shows a mixture of six- and five-sided polygons. This is likely to be closer to the real rock pattern than the regular assembly of hexagons found in some slowly cooled basalt flows. A quick examination of two easily treated regular patterns will show that any differences are likely to be very slight. Fig. 4(a) shows a uniform square grid

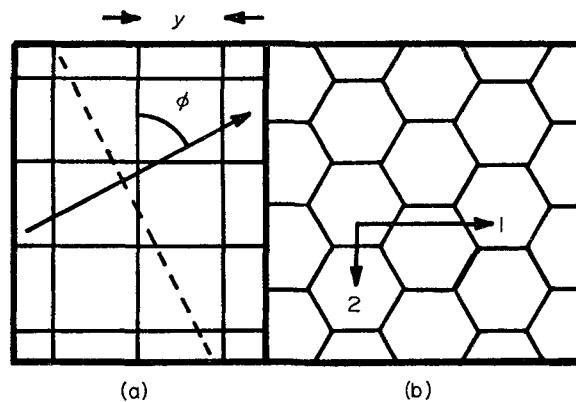


FIG. 4. Two different regular patterns of vertical cracks used for the calculation of permeability. The arrows represent possible horizontal flow directions, and the dashed line in part (a) indicates the crack counting plane normal to the flow. Both patterns have the same uniform horizontal permeability for a given  $y$ , and a vertical permeability twice as great.

of vertical cracks with the generalized direction of horizontal pressure and a crack-counting plane at right angles to it. The two sets of cracks can be considered separately and the permeabilities added in the resolved pressure gradient direction

$$D = \frac{d^3}{12} \left( \cos \phi \cdot \frac{\cos \phi}{y} + \sin \phi \cdot \frac{\sin \phi}{y} \right) = \frac{d^3}{12y}. \quad (35)$$

It should be noted that the permeability in the vertical direction is twice that in the horizontal direction for this case.

The hexagonal patterned case, diagrammed in Fig. 4(b), is most readily dealt with by calculating the effective permeability in two principal directions: one parallel to one set of hexagon sides, and one perpendicular to it. For direction 1, the permeability of the parallel cracks is just  $d^3/12y$ , and for the split flow through cracks at  $60^\circ$ ,  $D = 2(d^3/12y) \cos 60^\circ = d^3/12y$  again. In direction 2, the permeability of the zig-zag cracks is  $d^3 \cos 30^\circ/12$  and their mean separation is  $y \cos 30^\circ$ , so that the permeability is again  $d^3/12y$ . Since it is the same in 12 directions, it is again uniform in the horizontal plane, as might have been deduced directly from arguments of symmetry. The vertical permeability takes a little more calculation this time: the crack length attributable to each hexagon is  $\frac{1}{2} \cdot 6 \cdot \frac{1}{2}y \sec 30^\circ = \sqrt{3}y$ , while the area of the hexagon is  $\frac{1}{2}y^2 \sec 30^\circ + \frac{1}{2}y^2 \tan 30^\circ$  or  $(\sqrt{3}/2)y^2$ . The equivalent spacing for parallel cracks (one set) is therefore  $\frac{1}{2}y$ , and, again, the vertical permeability is twice the horizontal permeability.

Thus, for two quite different regular patterns, the horizontal permeability is  $d^3/12y$ , where  $y$  is the *effective intercrack spacing for thermal shrinkage*, and the vertical permeability is twice that. It is therefore likely to be an excellent approximation to assume that a quasirandom cracking pattern with a mean crack spacing of  $y$  will have similar properties. There is still a problem with the anisotropy of the cracked structure, since we shall be relying on experimental results for the heat transport at calculatable Rayleigh instability numbers. All the experiments used isotropic assemblies, usually of glass beads (Elder 1965), and so isotropic 'equivalent' permeability has to be estimated. A good arbitrary device is the geometric mean  $\sqrt{2}$ , since its presence in the formulae acts as a reminder that the assumption has been made.

It remains to calculate  $d$  in terms of temperature to obtain a useful formula. The zero for crack-widening shrinkage is the temperature at which the shrinkage stress equals the overburden pressure, since any additional shrinkage stress needed to cause the cracks to propagate is relieved elastically as soon as they have passed the point of interest. So we may write

$$d = \alpha y (T_\phi - T_w) - \frac{1}{2} \epsilon_\phi y \quad (36)$$

and finally

$$D = \frac{\sqrt{2}y^2}{12} [\alpha (T_\phi - T_w) - \frac{1}{2} \epsilon_\phi]^3, \quad (37)$$

where a creep term is retained in case the temperature drop from  $T_\phi$  to  $T_w$  is not sufficient to fully freeze the deformation. The fact that permeability increases rapidly with crack spacing can be anticipated from the conclusions of Bodvarsson & Lowell (1972), but, most important, is the tendency for the system to equilibrate. The front velocity is increased by increased permeability, but this lowers the crack spacing and therefore the permeability, leading to a stable equilibrium.

## 8. Convection

The fundamental experimental results on the rate of heat transport through a permeable slab have been summarized by Elder (1965, Fig. 15). The thermal flux is

increased over the conductive flux at the same temperature difference by a factor called the Nusselt number, and, as long as the flow remains laminar

$$\mathcal{N} = \frac{\mathcal{A}}{\mathcal{A}c}, \quad (38)$$

For a horizontal, parallel-sided slab, the critical Rayleigh number is  $40 \simeq 4\pi^2$  in agreement with the theoretical prediction of Lapwood (1948). Using the form of Rayleigh number appropriate to porous-medium convection, the total heat transport can be written down

$$\mathcal{A} = \frac{Da_w g \Delta T h}{\kappa' v_w} \quad (39)$$

$$Q = \frac{\mathcal{N} \kappa \rho c \Delta T}{h} = \frac{Da_w \rho c g (\Delta T)^2}{40 v_w}. \quad (40)$$

Many of the quantities in this result will vary with height through the convecting slab, and even with position in the cells. Taking them one at a time, the most important permeability is that near the heated surface: measurements in cells whose flow was modified by siphoning-off water showed that  $\mathcal{N}$  was unchanged despite radical changes in the flow pattern (Elder 1965). Therefore the water temperature that should be used in calculating  $D$  is the temperature of the *hot* column fluid as it collects near the hot surface. Experiments in free convection with a variable viscosity fluid (Booker 1972) show that the heat transport is insensitive to the changes in flow pattern caused by variable viscosity, and that the viscosity at the mean temperature may be used. Now, the least viscous fluid is in the least permeable rock (37), and it has been demonstrated by experiment that the conditions near the heat source are the most important for percolation convection. So it is probably safe to choose the *hot water* viscosity for calculation of heat transport in this case. No experiments seem to have been done with fluids of variable expansion coefficient, and water does have a variable coefficient in the range of interest, but the argument of insensitivity to conditions away from the heat source may be used again to justify choosing the expansion coefficient of the hot water. In any case, the effect of variations in water properties is small compared to the changes in permeability (37).

The most difficult problem is what to choose for the lower boundary temperature, since the permeability is zero from  $T_\phi$ , and the actual conductive source temperature is  $T_K$ , somewhat less than  $T_\phi$  but larger than  $T_w$ . The permeability is a very strong function of the cooling shrinkage, and it may be wise to choose the temperature at which the permeability has been reduced to half

$$(T_\phi - T_2)^3 = \frac{1}{2}(T_\phi - T_w)^3 \quad (41)$$

whereupon

$$T_2 \simeq \frac{(8T_w + T_\phi)}{9}. \quad (42)$$

Now, the rock is cooled from  $T_1$  to  $T_w$  in the process of passage of the cooling front, and the heat liberated per unit area is

$$Q = u\rho c(T_1 - T_w) \quad (43)$$

assuming that the rock specific heat is constant enough over the range of temperature to be assigned a single value. The heat capacity of the porous medium will differ

very little from that of uncracked rock, since the porosities due to thermal contraction are at most a few per cent, and the heat capacity of the interstitial water is not very different from that of rock on a volume basis. So, to an order of accuracy quite good enough for this analysis, we may solve for  $u$  from (43) and (40)

$$u = \frac{D\alpha_w g(8T_w + T_\phi - 9T_0)^2}{3240v_w(T_1 - T_w)} \tag{44}$$

Equation (37) gives  $D$  in terms of the crack spacing  $y$ , and a relationship between  $u$  and  $y$  has already been obtained in (31) by looking ahead at the results of the next section. Combining (31), (37) and (44), and neglecting the effect of  $\varepsilon_\phi$ , we obtain

$$u^{2.6} = \frac{\sqrt{2} \times 16^{0.8}}{12 \times 3240} \cdot \frac{\phi^{0.8} \kappa^{1.6} \alpha^3 \alpha_w g}{v_w} \cdot \frac{(T_\phi - T_w)^3 (8T_w + T_\phi - 9T_0)^2}{(T_1 - T_w)(T_1 - T_k)^{0.8}} \tag{45}$$

where  $u$  is seen to be most sensitive to  $(T_\phi - T_w)$  and  $(T_w - T_0)$ , among the undetermined factors. The difference  $T_\phi - T_k$  is small for reasonable values of  $\phi$  and  $y$  (30) and therefore it is permissible to substitute  $T_\phi$  for  $T_k$  in (45). If this is done, and  $T_\phi$  can be specified by reference to creep properties, the remaining unknown is  $T_w$ . The water temperature can be considered as a subsidiary variable, since there are good physical reasons to expect it to adjust itself to maximize  $u$ . If the water is too cool, the permeability is high and water has better access to the cracking front, accelerating it and heating up the water. If the water is too hot and moving slowly in a low permeability matrix, colder water is able to penetrate the hot regions by virtue of its greater mobility, thus cooling down the system. The stability of the equilibrium is modified somewhat by the actual heat-transfer mechanism at the boundary cracking front, but any attempt at discussing that has been eschewed for this paper. Convective regimes are usually stable statistically, even when a freely convecting fluid has a strong negative or positive temperature coefficient of viscosity. There is no reason to expect that the coupling of permeability with temperature will affect the attainment of a stable equilibrium in this system, especially as it opposes the viscosity variation in the percolating water.

The water temperature that maximizes the penetration rate can be found from

$$\frac{\partial u}{\partial T_w} = 0$$

$$32T_w = (20T_1 + 3T_\phi + 9T_0) - [(20T_1 + 3T_\phi + 9T_0)^2 - 32(27T_1 T_0 + T_\phi^2 - 9T_\phi T_0 + 13T_1 T_\phi)]^{\frac{1}{2}} \tag{46}$$

and this value, together with the parameter values listed in Appendix I, allow  $u$  to be calculated:

$$u^{2.6} = 7.644 \times 10^{-24} \phi^{0.8} \frac{(T_w - 273)^2 (T_\phi - T_w)^3 (8T_w + T_\phi - 9T_0)^2}{(T_1 - T_w)(T_1 - T_\phi)^{0.8}} \tag{47}$$

The  $\alpha_w/v_w$  component of  $T_w$  was not included in the maximization because it would probably represent an overdependence on the hot column conditions and also because the properties of water may be less temperature dependent at a pressure of 1 kb.

A little table of the various results for different choices of  $T_{\phi}$  can be constructed.

**Table 1**

$T_{\phi}$	500	600	700	800	900	1000	°K
$T_W$	350	386	423	462	502	544	°K
$u\phi^{-0.31}$	1.65	4.7	10.2	19.3	33	54	$\times 10^{-5} \text{ cms}^{-1}$
$u\phi^{-0.31}$	5.2	15	32	61	104	170	m/yr
$x_0\phi^{0.31}$	545	190	88	47	27	16.7	cm
$y\phi^{-0.15}$	30	13.3	7.5	4.8	3.3	2.4	cm
$\dot{\epsilon}_{\phi}\phi^{-0.62}$	0.9	6.6	28	87	220	490	$\times 10^{-9} \text{ s}^{-1}$
$D\phi^{-0.3}$	12	6.9	4.8	3.5	2.7	2.2	$\times 10^{-7} \text{ cm}^2$
$Q\phi^{-0.31}$	0.6	1.7	3.5	6.4	10.6	17	kw m <sup>-2</sup>

The 'fudge factor'  $\phi$  for the cracking stress has been retained, and it appears as a low enough power in most of the entries to give some assurance that the results are roughly correct. The parameter most affected,  $\dot{\epsilon}_{\phi}$ , is the one of least effect if an important basic result of Table 2 can be believed: that the rate of stress rise with decreasing temperature is little affected by creep rate in the medium stress region.

The most salient results of the analysis are that the crack spacing is in the range of a few centimetres, most definitely not at the kilometre spacing suggested by Bodvarsson & Lowell (1972) or on the sub-millimetre scale on which ultramafic rock fabrics are organized (Coleman & Keith 1971). The velocity of front advance is remarkably high, several orders of magnitude higher than sea-floor spreading velocities, and hydrothermal temperatures are within the range of those observed. The permeabilities are high compared to those usually observed in surficial geothermal flow, but the idealized conditions considered in the model are considerably different from those usually found in continental geothermal areas, and from those actually present on an oceanic ridge (as will be discussed). The creep rates near the cracking front cover the widest range, and sensitize the solution of cracking temperature to the creep model used. We are now ready to consider the problem of medium temperature rock creep with a clear idea of what to look for.

## 9. Creep

The phenomenon of creep in rocks is a complex and difficult subject and it will be tackled with objectives substantially short of the impractical goal of full understanding. The circumstantial evidence already introduced (Lister 1972; Ward 1972), together with equation (10) show that the creep we are interested in is very different from the high-temperature steady-state variety usually treated in the geophysical literature (*cf.* Weertman 1970). Specifically, the region of interest is the medium temperature, medium stress range of *transient* creep, since total strains of 8 per cent or more are needed to approach a steady state even at high temperature (Carter & Ave'Lallement 1970). These authors publish loading curves for specimens of dunite and lherzolite at constant deformation rates, high confining pressure, varying temperature and unknown water vapour pressure. Experimental difficulties associated with the geometry of the apparatus, such as the elastic response of the set-up, the piston friction, and the non-zero strength of the solid confining medium (talc) make the numerical values somewhat suspect (J. D. Blacic, private communication). The gross qualitative results, particularly the comparisons between similar runs at moderately varied temperature and strain rate, should not be unduly affected by the problems

just mentioned. We shall so assume, and examine whether the salient features of the dependence of stress on temperature and strain rate correspond to any reasonably plausible physical theory.

The most striking features of the data presented by Carter & Ave'Lallement (1970, Fig. 7, p. 2193) are the relatively modest increases in stress corresponding to temperature decreases in the 600–1200°K range, at constant strain rate, and the tendency for stress variation with strain rate to become small at the lowest temperatures and lowest strain rates for which comparative data are presented. If a temperature-activated process controls the creep, the first result suggests an exponential stress dependence, such as is provided by the old sinh creep law at high stresses. It may be useful to examine the physics of that law, as it was proposed by Ree, Ree & Eyring (1960) to explain the creep of soft metals at moderate temperatures. These are conditions where dislocation glide is probably the dominant creep mechanism.

In rock materials at high temperatures, and in steady-state creep, dislocations have to be generated, disposed of and permitted to avoid obstacles. Their collection in kink-bands causes grain subdivision and eventual recrystallization (Green & Radcliffe 1972), and the rate limiting process is the diffusion necessary for dislocation climb. In the initial stages of strain, however, plastic flow can take place by the glide of pre-existing dislocations on the planes permitted by the crystal structure, provided that the grain orientation of the rock is either sufficiently disordered or favourably oriented. It is not yet clear how mechanically anisotropic an olivine-bearing rock can be, so let us simply test the assumption that a thermally activated dislocation glide is associated with transient creep without introducing anisotropic complexities. The thermally activated transition could be the one step glide of a dislocation, or it could be passage past a (relatively rare) 'bad site' as proposed by Ree, Ree & Eyring (1960). In either case, creep is caused by the difference in the forward and reverse flow rates of the transition induced by the stress

$$\dot{\epsilon} \propto \left[ \exp\left(\frac{-H + \Omega\sigma}{RT}\right) - \exp\left(\frac{-H - \Omega\sigma}{RT}\right) \right] = \exp\left(-\frac{H}{RT}\right) 2 \sinh\frac{\Omega\sigma}{RT}. \quad (48)$$

This simple calculation is the basis of the old sinh creep law, and such a law does appear to fit the data for soft alloys quite well, especially when populations of bad sites with different activation energies are permitted (Ree, Ree & Eyring 1960). The metal data do seem to fit better to a law containing a constant stress multiplier in the sinh term than one that depends on temperature, and few empirical creep laws contain a significantly varying function of  $T$  outside of the activation exponential. The above authors go to some lengths to try to justify the variation of activation volume  $\Omega$  with temperature, but neither of the arguments used appears to be physically sound. Since the theory is at best an extremely crude approximation to the complexities of transient creep, and the temperature variations in the range of interest would modify the calculated  $\sigma$  by less than a factor of two, we shall follow the above authors and see what can be done with a relation of the form

$$\dot{\epsilon} = E \exp\left(-\frac{H}{RT}\right) 2 \sinh\frac{\sigma}{\sigma_0}. \quad (49)$$

During compression at a constant strain rate, the stress rises from zero toward a quasi-linear asymptote with a non-zero intercept at zero strain. Even at a constant temperature, the curve is the result of complex processes, such as the gradual locking of movable dislocations, and the unfavourable rotation of slip planes that started at orientations favourable to the relief of the applied stress. Each component of the stress should follow a geometrically controlled law that has the same form over a

**Table 2**  
*Stress at 1 per cent plastic strain: wet hercynite*

Temperature		Strain rate: s <sup>-1</sup>						
°C	°K	7.8 × 10 <sup>-4</sup>	7.8 × 10 <sup>-5</sup>	7.8 × 10 <sup>-6</sup>	7.8 × 10 <sup>-7</sup>	7.8 × 10 <sup>-8</sup>	7.8 × 10 <sup>-9</sup>	7.8 × 10 <sup>-10</sup>
325	598	(3.3 + 12.0)	9 (3.1 + 10.4)	(3.0 + 9.2)	(2.8 + 7.9)	(2.6 + 6.5)	(2.5 + 5.1)	(2.3 + 3.7)
	700	(2.6 + 9.1)	(2.4 + 7.7)	(2.3 + 6.3)	(2.1 + 5.0)	(1.9 + 3.6)	(1.8 + 2.2)	(1.6 + 0.8)
	800	(2.1 + 7.0)	(1.9 + 5.6)	(1.8 + 4.2)	(1.6 + 2.8)	(1.4 + 1.5)	(1.3 + 0.32)	(1.1 + 0.03)
635	908	(1.7 + 5.2)	5.5 (1.5 + 3.8*)	(1.3 + 2.4)	(1.2 + 1.0)	(1.0 + 0.16)	(0.86 + 0.016)	(0.7 + 0.0016)
740	1913	(1.35 + 3.8)	3.8 (1.2 + 2.4)	(1.0 + 1.0)	(0.9 + 0.16)	(0.7 + 0.016)	(0.55 + 0.0016)	(0.39 + )
850	1123	(1.1 + 2.6)	2.3 (0.9 + 1.3)	2.5†(0.8 + 0.24)	(0.6 + 0.03)	(0.4 + 0.003)	(0.27 + )	(0.11 + )
950	1223	1.7(0.9 + 1.7)	1.2 (0.7 + 0.5*)	0.8 (0.55 + 0.055)	(0.4 + 0.005)	(0.2 + )	(0.08 + )	(0.009 + )
1060	1333	1.2(0.7 + 0.2)	0.55(0.5* + 0.02)	0.35(0.36* + 0.001)	(0.2 + )	(0.06 + )	(0.006 + )	(0.0006 + )
1170	1443	0.8(0.5 + 0.05)	0.34(0.37 + 0.005)	0.2 (0.21 + )	(0.06 + )	(0.007 + )	(0.0007 + )	( )

$$\text{Column entry: data} \left( 0.07 \operatorname{arc} \sinh \frac{80}{RT} \right) \left[ \frac{1}{2} \left[ \dot{\epsilon} \exp(-8.9) \exp \left( \frac{80}{RT} \right) \right] + 0.6 \operatorname{arc} \sinh \frac{1}{2} \left[ \dot{\epsilon} \exp(-2.1) \exp \left( \frac{40}{RT} \right) \right] \right] \quad (50)$$

with data from Carter & Ave Lalleme (1970).

\* Indicates value chosen to fit formulae to data; activation heats assumed.

† Value referred to in the text: not consistent with the other data.



considerable range of temperature, and, to a first approximation, one might assume that the form of the total stress curve remains essentially similar also. It is then possible to compare stress level variations with temperature and strain rate by tabulating the stress at a particular arbitrary amount of strain, preferably far enough up the curves to provide good stress resolution, but not too close to the asymptotic region where gross changes in mechanism are known to occur with varying temperature (Green & Radcliffe 1972). The *stress at 1 per cent strain* has been picked off the loading curves of Carter & Ave'Lallement (1970) and the values listed in Table 2. Elastic shortening of the specimens has been corrected for at the higher stress levels, so that the figures represent 1 per cent of *plastic* strain; a modulus of 1.5 Mb was used. If more than one stress value could be picked off the graphs for given conditions, the figures have been averaged.

The theoretical modelling has followed the technique of Ree *et al.* (1960) in expressing the total stress as the sum of components needed to drive dislocations past different kinds of obstacle. One is spatially rare, has a low activation stress but a high activation energy and probably corresponds to major obstacles to glide such as must be overcome in 'steady-state' creep at high temperatures. An activation energy comparable to that obtained by Carter & Ave'Lallement (1970) for the high-temperature creep of wet lherzolite is therefore appropriate, and their value of 80 kcal/mole has been used. The second stress component has a high activation stress corresponding to something much more common in the crystal grains, but a relatively low activation energy. It is probably an energy associated with the activation of glide itself, and a guesstimate value of 40 kcal/mole has been used (J. D. Blacic, private communication). This is considerably higher than that determined for the water-activation of quartz (*cf.* Martin 1972) but may be reasonable for olivine.

The fit of the theoretical results to the data is tolerable, except for the value indicated by a dagger in the table that could not be fitted by any physically reasonable formula, and the gradation of values at the highest strain rate. It should be noted that no attempt was made to obtain any kind of least-squares fit to the data, since the extrapolation of such a fit to much lower strain rates is crucially dependent on the accuracy of the experiments themselves, and obviously unwarranted because of the internal inconsistency of the values. Rather, the formulae were fitted to reasonable-looking values in the regions where the sensitivity of the fit is good, and simply allowed to extrapolate elsewhere. *Qualitatively*, at least, the fit is reasonable, considerably better than could be achieved by any power law of creep limited in degree, and even better than the fits obtained by Carter & Ave'Lallement (1970), to their formula for high temperature creep. If one can accept the physical basis as reasonable, then the extrapolation to low strain rates such as those estimated by (38) may be at least *qualitatively* correct. At stresses of about 1.4 kb and strain rates of about  $3 \times 10^{-8} \text{ s}^{-1}$ , the table suggests that the first term is dominant. If this is so, then the *stress at 1 per cent strain* is proportional to the *logarithm of the strain rate and to inverse temperature*, in other words is a slowly varying function of these parameters in the range of interest. If this conclusion can be extended to the case of thermally induced contraction creep, where the temperature varies continuously, then the assumptions made in the previous sections will have been validated qualitatively.

One other aspect of the creep data should be discussed before the quasi-theoretical model is used to conclude the argument. It has been noted above that the second most striking feature of the transient strain data is the tendency for stress variation with strain rate to become small for low strain rates and low temperatures. An extreme example of this is the data point indicated by a dagger in Table 2, where a tenfold drop in strain rate results in an *increased* stress. Specimen-to-specimen variation has something to do with this particular example, but there does seem to be a trend, and it has been carefully fudged in the theoretical fit by making use of the logarithmic to linear transition of the second (low activation energy) term in the

formula. Now, the effect *could* be done to frictional effects in the apparatus (temperature dependent) either on the mechanical parts themselves or through the properties of the confining medium, but there is another physical mechanism of some importance that has been neglected so far.

In order to induce a substantial stress between a dislocation and an obstacle, a finite amount of deformation must be applied. In simplified geometrical terms, the dislocation is like a piece of cord that cannot apply a sideways force unless it is bent around an obstacle and put into tension. Until the dislocation passes the obstacle, the applied deformation is reversible as it has been absorbed in elastic deformation of the dislocation in the crystal lattice: if the applied stress is relieved, the dislocation will creep back to a lower energy configuration at a rate determined by the glide activation. The phenomenon is thus akin to a kind of slow-response elasticity, and is responsible for the partial recovery of plastically strained materials. This is not a paper on creep, and so no attempt has been made to account for this phenomenon in the theoretical formulae. The physics of the effect should, however, be noted for the case of interest: decreasing temperature and increasing strain rate leading to a steadily growing stress. *Some* of the plastic strain is being absorbed by this quasi-elastic process to load the high activation-energy obstacles, and the stress reduction is significant whenever the glide stress (second term) is small compared to the obstacle-climbing stress (first term). We have already noted that this is likely to be the case in the region of interest. How large is the strain involved? One piece of data that may give a clue is the sequence of different strain rates applied to a specimen in the plot of Fig. 7(e) of Carter & Ave'Lllement (1970). The temperature is too high, and the strains go well into the steady-state region, but the recovery of stress when the strain rate is stepped back up takes about 1 per cent strain to rise 1.4 kbar. This may indicate the order of magnitude involved: if it does, then the two-term fitting equation we have used gives too large a stress contribution from the first term at the higher stresses.

The figure just cited is also of value in extending the isothermal creep results to the real case of steadily varying temperature. It suggests that, subject to the strain needed to build up local stresses at obstacles, the geometrical effect of total strain is *essentially independent of the conditions under which it was built up*. Thus, when the deformation rate is stepped back up to its initial value, the stress rises rapidly back onto the original stress curve, not onto a new curve with a displaced (yielded) origin. As the temperature of the rock falls and strain takes place due to thermal contraction, the stress will always be tending toward the isothermal stress at the latest temperature, strain rate, and *total strain*. The lag will be entirely due to the mechanism discussed just above: the finite amount of strain needed to place piled-up dislocations under activating stress. Note that there should be no lag as far as the second term, the glide activation, is concerned. Now, if the initial temperature is 1500 °K, the total plastic strain to 800 °K is approximately 2 per cent equivalent linear strain. The stress at 1 per cent strain, creep rate of  $3 \times 10^{-8} \text{ s}^{-1}$ , is about  $(1.35 + 0.8) = 2.15 \text{ kb}$  according to the extrapolated formula, neglecting the build-up strain required by the first term. At 2 per cent total real strain, the first term will have the necessary build-up strain, while the second term will be somewhat larger because of the more adverse geometry. The predicted stress should be of the order of 2.4 kb. At 900 °K, total strain of 1.8 per cent, and similar strain rate, the stress would be about 1.0 kb, and at 1000 °K about 0.6 kb. Therefore, over a considerable range of overburden pressure, or depth in the oceanic crust, the cracking temperature should remain in a relatively narrow range, 800–1000 °K. Reference to Table 1 shows that the velocity of advance of the cracking front should remain in the range of 60–200 m/yr and the somewhat higher strain rates affect the stress estimates only slightly. The temperature of the hot hydrothermal water should be about 480 °K when the depth of penetration is 7 km.

These figures are all plausible values, and give some confidence that the approach

we have used is qualitatively reasonable. It should be noted, however, that the creep extrapolation gives no indication that water penetration should cease at some depth like 7 km, corresponding to a known seismic-velocity boundary (the Mohorovicic discontinuity). At the strain rates calculated, the stress could rise easily to levels of 6 kb, corresponding to depths of 30 km in the mantle, provided that the water-passage cracks remain open and the front continues to advance. Under what conditions the cracks *do* remain open remains to be discussed, and there are several mechanisms of closure that must be considered: continuation of creep under the overburden stress; elastic instability of the columnar structure; static fatigue of the rock material; and hydrothermal alteration and swelling of the rock itself.

## 10. Creep after chilling

The first potential mechanism for reducing or terminating water percolation is the continued creep of the overburden-supporting rock columns in their water-cooled condition. Before considering the rock behaviour at the water temperature, it is necessary to show that the continued creep during the cooling period is negligible. At the cracking temperature, the creep rate caused by the overburden pressure is already less than the creep rate forced by the cooling, since this is the condition that permits cracking to occur. The transient creep would slow down with time even at a constant temperature, and so a highly conservative estimate of continued creep would consider only the slowing down of the creep process due to decreasing temperature. Again, the most conservative estimate is that using the lowest activation energy, and this is 40 kcal/mole in (50). An order of magnitude ( $10^{-1}$ ) decrease in rate occurs for a temperature change of only 70 °K near 800 °K, even at this low activation energy. Therefore, even if the cooling rate does not accelerate behind the cracking front, as it should according to the model, the creep rate becomes negligible compared to the thermal shrinkage rate after a mere 70 °K of further cooling. Plausible hydrothermal temperatures of 400 to 500 °K are more than 300 °K below the cracking temperature (Table 1), and therefore the fraction of the thermal shrinkage lost to continued creep (36) can be neglected safely at the order of accuracy of these calculations.

The rock is now at the circulating water temperature, and some numerical estimate must be made of the continuing creep rate. The creep data that have been used to construct Table 2 are for stress at constant strain rate, and are not strictly applicable to the entirely different case of strain at constant stress. Relaxation phenomena generally follow logarithmic time dependence laws, where the rates are inversely proportional to elapsed time, so that some estimate of the initial reference time must be made to go with a guess at the creep rate. This suggests a way of using Table 2 to derive a value of the strain rate at a constant stress. Let us suppose that a specimen at the temperature of interest has been strained at a constant rate until a certain stress has been built up, and that now the strain rate will be adjusted so as to keep the stress constant. The physical continuity of the experiment demands that the initial strain rate must be equal to the previous constant value, and it would be surprising if the reference time were very different from the time it has taken to strain the specimen to the required stress. Now consider the chilled rock: it has been strained a certain amount and is now under a certain stress. Provided that the dislocation slip geometry resulting from the higher temperature strain is similar to that produced by slower creep at the low temperature, there is little to distinguish the chilled rock from rock that has been strained at the low temperature by the same amount. So we can look into Table 2 for the strain rate that would produce the overburden stress at 1 per cent strain and the new chilled temperature, and take this as a reasonable guess at the strain rate we require. The formula associated with the table has two terms, and the

first is the stronger function of temperature and the weaker function of strain rate. This term should dominate at a low-temperature and low strain rate condition, so that the vertical uniaxial strain rate

$$\dot{\epsilon} \approx \exp(8.9) \exp\left(-\frac{80}{RT}\right) 2 \sinh\left(\frac{\sigma}{0.07}\right) \approx \exp\left[8.9 - \frac{80}{RT} + \frac{\sigma}{0.07}\right]. \quad (51)$$

At the expected conditions of  $T \approx 450^\circ\text{K}$  and  $\sigma = 1.4 \text{ kb}$ , the initial strain rate should be about  $10^{-26} \text{ s}^{-1}$ , and the reference time for relaxation is the 1 per cent or so of actual strain divided by that, or about  $10^{24} \text{ s} \approx 3 \times 10^{16} \text{ years}$ .

Now the crack opening corresponds to a uniaxial strain of about 1 per cent and the bulk rock permeability would be reduced by half upon a uniaxial relaxation of about 0.2 per cent because of the cube law. Since the reference time was calculated for 1 per cent strain, a steady strain rate can be assumed for the relaxation, and the time to half permeability estimated as

$$\tau \sim 0.002 \dot{\epsilon}^{-1} = \exp\left[\frac{80}{RT} - \frac{\sigma}{0.07} - 15.1\right]. \quad (52)$$

For the above conditions  $\tau \sim 2 \times 10^{23} \text{ s} \sim 7 \times 10^{15} \text{ years}$ . Even if the actual initial creep of the freshly chilled material is considerably faster than that of material strained at the lower temperature, the creep is unlikely to be significant in geological time. The actual estimate is dependent on the doubtful data and formula from Table 2, but the result can be generalized for any material with a comparable creep activation energy: if it is stiff enough to crack at  $800^\circ\text{K}$ , then residual creep at  $450^\circ\text{K}$  is going to be negligible. Only at the highest imaginable hydrothermal temperatures does the mechanism of continued creep influence permeability in times short enough to be of interest. For example, at  $600^\circ\text{K}$  the permeability would fall to half its initial value in about 1 My, but such high temperatures have only been observed in shallow, volcanism-related, geothermal areas (Elder 1965).

## 11. Elastic stability

Consideration of the planar percolation model has led to the concept of a rock matrix divided into an assemblage of quasi-hexagonal columns. They should be a few centimetres in diameter and separated by predominantly vertical cracks. If these columns were continuous for several metres they could hardly support the overburden stress without becoming unstable to elastic buckling. The sheer number of the columns does not improve the stability of the assemblage, as they would all buckle in concert like the fibres of a rope put into compression. Only if the cracks deviate sufficiently from a regular vertical pattern can such an assemblage be stable: the structure is cross-braced by the intercalation, merging and division of the columns. The actual amount of cross-bracing needed for stability could be estimated, at least in principle, and expressed, say, as a lateral rigidity to low frequency deformations. Such a study in elasticity theory is beyond the intended scope of this paper, and this section will conclude with a mere indication of the way in which bracing may be generated.

It has been pointed out already that the columnar structure is inherently somewhat irregular; it is also worth mentioning that the pattern of cracks depicted in Lachenbruch (1962) is a *surface lavaflow* set, not an arbitrary section through a three-dimensional body. The propagation of a geometrically regular set of cracks into a medium under planar tension could be stable; if the set were initially irregular it may remain geometrically unstable and irregular or it may tend toward a regular and stable pattern.

The question boils down to whether the overburden stress and buckling tendency can *cause* sufficient pattern instability to brace the assemblage well into equilibrium, or whether it remains marginal, indeed with columns elastically bent to close a number of cracks. Even this is not a simple problem, but one deduction can be made readily. Provided that no actual column destruction occurs, a limited amount of buckling or leaning of the columns should not affect the permeability. Little overall porosity would be lost, and for every crack that was closed another would be proportionately opened. The cube dependence of percolation on crack width would even suggest an increase in permeability after limited buckling, since the increase in the length of the easiest paths would not be enough to counteract the reduced flow resistance. Perhaps the best approach is to accept the field evidence for percolation and the presence of micro-, not macro-, earthquakes as confirmation that sufficient bracing does occur, and simply note that, since creep essentially stops after chilling, an assemblage that was stable initially is likely to remain so.

## 12. Static fatigue

When a brittle material is placed under stress very little dislocation creep takes place, as we have seen in the case for rock at hydrothermal temperatures. Instead, after some interval of time a sudden and total failure of the specimen occurs. Data and mechanisms for *tensile* failure are fairly well established in the literature, especially for glasses (*cf.* Hillig & Charles 1965), but the mechanism for failure under compressive stress must be quite different. Under tensile conditions, the propagation of cracks into the material both reduces the load-bearing cross-section and rapidly increases the stress magnification at the crack tips. In compression, however, the cracks can only propagate parallel to the applied stress, and the result is a steadily diminishing stress concentration (Martin 1972). Data obtained by Scholtz (1972) on the microfracturing rate of stressed single-crystal quartz support this mechanism concept: the rate decreases steadily after the application or increase of stress. Nevertheless, the samples explode after a period of time. A solution to this apparent paradox is possible through the concept of columnar elastic instability, introduced in an earlier section for the assemblage of macrocracks generated by the water percolation. Internal microfracturing, probably invisible except by means of an ultramicroscope (Scholtz 1972) gradually divides the load-bearing cross-section into columns parallel to the applied compression. At some point the structure becomes elastically unstable and an exceedingly rapid and catastrophic collapse occurs, leaving the columns shattered into grains of sand.

The purpose of introducing a mechanism concept for static fatigue failure under compression is twofold. The first is to make it clear that catastrophic failure of this type can occur under the conditions we imagine to exist deep in the water percolation system. The second is to point out the probable result of failure: not only will the local porosity be decreased by the release of overburden stress, but the general fracture of the rock into small grains will decrease the permeability dramatically (*cf.* equation (37)). If we may indulge in a momentary speculation, the curious fabric structures observed by Coleman & Keith (1971) in a partially serpentized ultramafic outcrop are suggestive of a microfractured and crushed rock. If much later, very slow water penetration, serpentization, and rock expansion took place, the microfractured structure would be preserved by preferential alteration at water rock interfaces. The location of the Burro mountain outcrop in the Franciscan formation of the California coast ranges indicates that the rock was once part of the oceanic crust.

The only field evidence that static fatigue fracture may be taking place is the observation by Ward (1972) that micro-earthquake activity is associated with hydrothermal areas. These earthquakes cannot be produced by the cooling-cracking

mechanism associated with the water penetration itself, since the propagation of the tension cracks is stable on a macroscopic scale: advance of one crack reduces the tension at the tips of nearby cracks. By contrast, the failure of a column in static fatigue increases the stress on nearby columns and can induce the sympathetic collapse of a substantial volume. Neighbouring material should be at a similar stage of microfracturing to the column that goes first, and the degree of geometric crack separation within the structure necessary to create an elastic instability decreases as the ratios between the stress and the elastic moduli increase. The extent of the failure volume is probably limited by the variations in water-temperature history of rock in different parts of the hydrothermal convection cells. It is also important to note that the instantaneous displacement of the collapse is very small, since the increase in rock volume needed to separate the fractured grains can only come from the volumetric compression of the pore (= crack) water as its pressure rises momentarily from the hydrostatic to the lithostatic pressure. How efficiently a rock fabric may be destroyed in such a small volumetric change is not readily predictable, and it is unwise to speculate further on this until some adequately confined experimental runs have been made.

The chief difficulty in determining the static fatigue strength of an ultramafic or mafic rock is the acquisition of a specimen in as pristine a state as is available to the natural hydrothermal system. The laboratory strength of rock specimens is highly variable because they contain pre-existing cracks, strains and zones of weakness (*cf.* tables in Clark 1966), so that it is hardly surprising that most work on fatigue has been confined to glasses or single-crystal specimens. Since there appears to be no data on olivine or on any of the other common mafic minerals, we are reduced to discussing the data of Scholtz (1972) on the static fatigue of quartz. His results may be summarized in the following equations

$$\langle t \rangle \sim t_0 C_{\text{H}_2\text{O}}^{-\gamma} \exp\left(\frac{H' - \Omega'\sigma}{RT}\right) \sim t_0 C_{\text{H}_2\text{O}}^{-\gamma} \exp\left(\frac{H'}{RT} - \frac{\sigma}{\sigma'_0}\right) \quad (53)$$

where the material constants differ for the *a* and *c* axes in quartz. We will take the *c*-axis data and favour the second version of the formula in sympathy with the creep results, where stress activation appeared to be independent of temperature (Ree *et al* 1960). It is also advisable to follow Martin (1972) in using the active pressure of water vapour rather than the concentration as used by Scholtz (1972); replotting of the latter's Fig. 4 in terms of water pressure produces a unity power law dependence of the fatigue time consistent with the Martin formula (17). Finally replacing the stress exponential with a sinh term to obtain infinite life for zero stress, we arrive at

$$\langle t \rangle \sim t_0 P^{-1} \exp\left(\frac{H'}{RT}\right) \frac{1}{2} \sinh^{-1}\left(\frac{\sigma}{\sigma'_0}\right) \quad (54)$$

and numerically, using the constants determined by Scholtz (1972)

$$\langle t \rangle \sim \exp(-9.8)P^{-1} \exp\left(\frac{24}{RT}\right) \frac{1}{2} \sinh^{-1}\left(\frac{\sigma}{0.8}\right). \quad (55)$$

The conditions estimated for the zone of static fatigue failure as observed by Ward (1972) are  $T = 450^\circ\text{K}$ ,  $\sigma = 1.4 \text{ kb}$ , so

$$\langle t \rangle \sim \exp(14.8)P^{-1} \text{ s} = 0.1 P^{-1} \text{ years} \quad (56)$$

which is a remarkably short time unless the effective pressure of water vapour is small, or the mafic rock is much stronger than single-crystal quartz.

The estimation of the effective water vapour pressure in freshly penetrated crustal or upper mantle rock is difficult. There is no reliable information on the *in situ* water content of mantle material, since all ultramafic outcrops have been exposed to hydro-spheric moisture for times long enough to be penetrated thoroughly by hydroxyl diffusion from cracks and joints. Volcanoes emit steam and other volatiles, but extruded magma is highly concentrated in these relative to the original material and may be contaminated by contact with hydrated country rock. Furthermore, the hot rocks of prime interest here are the deeper layers of the oceanic crust, and these have been depleted in volatiles by the extrusive volcanism at the ridge crest. Not only is the water content hard to guess, but itself it is not sufficient to calculate the chemical activity pressure in the rock. Much of the moisture may be chemically bound by minerals, and the active concentration may even be a function of time since the rock is cooled into the stability fields of several hydrated minerals during the hydrothermal penetration itself. If the active concentrations were known, it would be easy to calculate the effective pressure for equation (56) by the gas laws; working backward, 1 bar at 450 °K would be produced by about 0.02 per cent water by weight at a usual mafic rock density. Since this corresponds to a life of only 0.1 year, and the cracking front would require 200 years to penetrate to 7 km at 34 m/yr, the rock must be either essentially anhydrous or much stronger than single-crystal quartz to permit a percolation regime to exist.

Before making use of equation (55) to estimate the level in the hydrothermal system at which failure may first take place, some consideration must be given to the diffusion of water into the columns, to see if this is or is not a limiting factor. Unfortunately, no data on aqueous diffusion rates appear to be available for mafic minerals, so the values obtained for quartz by Kats (1962) will have to suffice. There is some evidence (J. D. Blacic, private communication) that the activation energy for hydroxyl diffusion in olivine is somewhat larger than that in quartz, and this would suggest that diffusion rates in olivine may be lower at low temperatures. There is in any case one major imponderable between the calculation and the real situation: the effect of incipient microfracturing on the diffusion rate. If the microfractures formed a connected system, moisture could penetrate the rock at a rate orders of magnitude faster than that given by bulk diffusion. The data given by Scholtz (1972) on the response of his stressed specimens of quartz to the addition of water are not reassuring; the observed microfracturing rate reaches its new value in a few seconds. Fortunately he also says: ‘. . . close visual examination revealed that the surface of the sample was gradually becoming pitted and striated by many small elongate spalls. Small flakes, accompanied by crackling noises, were often observed to fly out from the specimen . . . Detailed examination failed to reveal any cracks deeper than the spall level, except in a few rare instances just before fracture of the specimen in which isolated axial cracks were observed to have penetrated up to 1 mm into the specimen’. If one may deduce that the ultrasonic microfracturing is associated with the visible surface spalling and not the invisible internal weakening, then the difficulty is resolved: surface spalling is instantly accelerated by adding water because all the cracks involved intersect the surface. Simple bulk diffusion is undoubtedly a lower bound to the rate of water penetration, but, since there is no reason to suppose the internal microfractures to be interconnected, the bound may be realistic enough to be worth calculating.

From Kats (1960) the diffusion rate for quartz is

$$F = F_0 \exp\left(-\frac{H''}{RT}\right) = 5.5 \times 10^{-5} \exp\left(-\frac{19.3}{RT}\right) \text{ cm}^2 \text{ s}^{-1} \quad (57)$$

and it can be assumed constant across the column for the purpose of making an order of magnitude estimate of the diffusion time. Further, the geometric complexities of

an irregular column can be avoided by assuming that the water pressure in the central region is about twice that found at a depth of two thirds the column radius from the surface of a halfspace

$$P_i \sim 2P_0 \operatorname{erfc} \left[ \frac{y}{6(Ft)^{\frac{1}{2}}} \right]. \quad (58)$$

Equation (56) is only applicable strictly to the case of constant water pressure, but it can be converted into an equation for instantaneous weakening rate

$$s = (1/\langle t \rangle) = P_i \exp(-14.8) \quad (59)$$

and failure under varying water pressure will take place when

$$\int_0^{\langle t \rangle} s dt = 1 \quad (60)$$

where  $\langle t \rangle$  is now the cumulative failure time under the changing conditions. Hence from (58), (59) and (60)

$$1 = \int_0^{\langle t \rangle} 2P_0 \exp(-14.8) \operatorname{erfc} \left[ \frac{y}{6(Ft)^{\frac{1}{2}}} \right] dt \quad (61)$$

and, using the substitution  $\xi = y/6(Ft)^{\frac{1}{2}}$

$$1 = \int_{\langle \xi \rangle}^{\infty} 2P_0 \exp(-14.8) \frac{y^2}{18F\xi^3} \operatorname{erfc}(\xi) d\xi. \quad (62)$$

Approximating this by the large-argument expansion of the error function from Carslaw & Jaeger (1959, p. 482)

$$1 \simeq \int_{\langle \xi \rangle}^{\infty} 2P_0 \exp(-14.8) \frac{y^2}{18F\pi^{\frac{1}{2}} \xi^4} \exp(-\xi^2) d\xi \quad (63)$$

and again taking the first term of the descending power series in  $\xi$  from successive integration by parts

$$1 \simeq 432P_0 \exp(-14.8) \frac{F^{3/2}}{y^3 \pi^{\frac{1}{2}}} \langle t \rangle^{5/2} \exp\left(-\frac{y^2}{36F\langle t \rangle}\right) \quad (64)$$

in the original notation. Substituting numerical values, for  $F$  from (57) at 450 °K, for  $y$  from (45),  $P_0 = 1000$  bars, and taking the logarithm

$$\frac{\exp(30.9)}{\langle t \rangle} - \frac{1}{2} \ln \langle t \rangle = -53.3 \quad (65)$$

a rough estimate of  $\langle t \rangle$  is obtained, finally, as

$$\langle t \rangle \sim \exp(28) \text{ secs} \simeq \frac{1}{2} \times 10^5 \text{ years.} \quad (66)$$

It should be reiterated that this is a gross estimate, based on data for quartz, not olivine, and neglecting many potentially operative physical mechanisms. Microfracturing could greatly accelerate the penetration of water, but trapping of moisture at sites where mineral hydration has nucleated could strongly impede it. The hydration itself and its attendant volumetric expansion (see discussion below) could accelerate



failure of the rock column by fracturing the rind, or it could seal off peripheral microfractures and further impede the penetration of water. These mechanisms are rock fabric, as well as mineral, dependent and can be studied only on representative materials. However, the order of magnitude of the answer is interestingly within the active range appropriate to the problem, and diffusion could only be neglected if the estimate of column width is of substantially, say by two orders of magnitude (or  $y = 4$  m).

It is useful to conclude by noting the relative sensitivity of the fatigue life to stress and temperature. Both mechanisms of failure, whether arising from moisture originally present, or by the diffusion of external moisture into stressed rock, are strongly temperature activated (54, 57). If the sinh formula is a qualitatively accurate representation of the stress dependence of static fatigue, variation in depth is of minor effect compared to variation in the temperature. For example, the equivalent of equation (56) at half the depth is

$$\langle t \rangle \sim 0.3P^{-1} \text{ years (3.5 km),} \quad (67)$$

while a similar lengthening of fatigue time could be obtained at 7 km depth by a mere 16 °K decrease in temperature. If static fatigue is the mechanism by which hydrothermal penetration is limited, no direct deduction of the depth of penetration can be made from the physics of the process. Unfortunately, the full boundary condition history of the system must be developed into a model before any clear conclusions can be reached.

### 13. Percolation boundary model

The hypothesis that static fatigue is the limiting phenomenon for hydrothermal penetration can be developed into a model only with a concept of the macroscopic failure mode. It has already been mentioned that the shattering of the rock columns into sub-millimetre fragments must greatly diminish the permeability of the matrix, but is the failure a true bulk phenomenon? Hydrothermal convection on a kilometre scale can be impeded seriously only by permeability loss on a similar scale, or at least by the formation of a relatively impermeable layer of substantial thickness. It is encouraging that significant microearthquakes exist at depth in a geothermal area, as reported by Ward (1972): the mechanical energy available per unit volume of failure is small, due to the small displacement possible, so the failure volumes should be relatively large. Here follows an elementary treatment of the mechanical problem, and an attempt to justify the idea that substantial volumes of rock should lose their permeability in the process.

When a rock specimen fails in a compression testing machine, some of it turns into a powder, either in a narrow vein along the shear fracture plane or over most of the central region. Much of the energy involved in the shattering is stored elastically in the testing machine, and the specimen is relatively unconfined laterally because of the mechanical softness of the usual systems for applying confining pressure. In the natural case, the surrounding rock provides considerable confining rigidity, but it is also under stress and may be triggered into failure. The important question, therefore, is how failure should propagate from a small region of initial collapse in a matrix that is all under stress and close to failure over a substantial volume: is the pulverized region confined to an extensive but thin sheet at a favourable shear angle, or does volumetric destruction take place?

The situation is sketched in Fig. 5: a quasi-circular region at the shear angle has failed and contains a small but finite thickness of pulverized material containing pore water at the lithostatic pressure. Rock above and below the region is subjected to horizontal pressure, decreasing the water pressure in the cracks on one side and

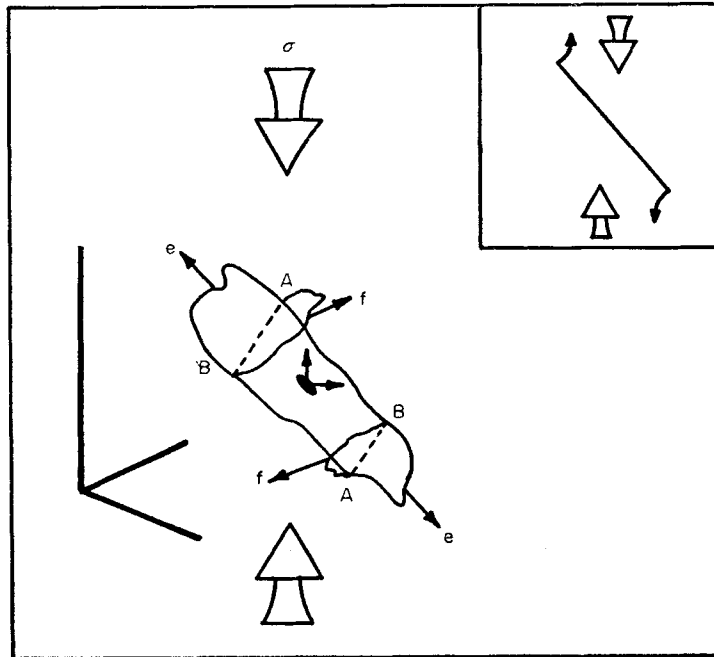


FIG. 5. Geometric diagram of a static fatigue failure region and its probable directions of propagation. The effect of the excess hydrostatic pressure associated with the failure is indicated by the small arrows leading from the filled oval. Letters describing the four principal regions (capitals) and potential propagation directions (lower case) are referred to in the text. The inset depicts the direction of crack propagation in a  $45^\circ$  faulted material under compressive stress.

increasing it on the other. Thus, pore pressure in the large volumetric regions A is drastically reduced, while that in regions B rises towards the lithostatic pressure. The regions A now have a much greater deviatoric stress applied than before and should fail at once: the zone of peak deviatoric stress is slightly *behind* the edge of the original failure disc, and the most favourable direction of failure propagation is f and not e. This is analogous to the direction of propagation of a tension crack if material with an inclined slit is subjected to compressive stress (R. J. Martin, private communication) as is indicated by the inset to Fig. 5. *It is most important to note that the situation depicted here is quite different from that associated with sliding fractures in a region of horizontal shear stress, such as the San Andreas fault* (Nur & Booker 1972). There, a decrease in pore pressure increases the normal force on potential sliding surfaces, and thus their frictional strength; here, the decrease in pore pressure increases the deviatoric stress directly and enhances failure. It is clear that the single inclined shear zone is not an expected result of failure: the tendency of elastic failure to branch off in conjugate directions should ensure a quasi-volumetric result. How much of the final region is shattered, and how much merely contains the original matrix horizontally compressed, depends upon several unknown properties of the cracked matrix itself: principally its horizontal compressibility and vertical shear rigidity. The shape of the volume of failure depends on these, and also rather critically on the distribution of fatigue weakened rock and the sensitivity of partially fatigued rock to overstress.

It is probable that the final failure region would include the whole lateral area of rock in a hot upwelling convection plume, and have a vertical extent limited either by the temperature variation or the vertical shear rigidity of the nearby matrix: the tendency for a large surrounding area to take up the excess overburden stress. Some

of the stress is distributed immediately because of the small but finite displacement involved in failure, the volume decrease as the pore fluid rises from the hydrostatic to the lithostatic pressure. More is applied later as the high pressure pore fluid leaks away and further settling takes place. This latter process should give rise to micro-earthquake swarms, in a way somewhat analogous to horizontal shear aftershock swarms (Nur & Booker 1972) but actually more direct. The deviatoric stress is directly related to the pore pressure, and each new failure locally increases it back to the lithostatic pressure. Thus, the frequency of the shocks from a single localised source region should be a measure of the region's percolation time constant, the principal unknown being the level to which the pore pressure must drop to permit further failures. This is another example of the importance of the sensitivity to instantaneous stress of weakened rock, at present totally unknown.

According to the preceding arguments, the static fatigue failure should substantially reduce the permeability of rock over the whole cross-section of an upwelling hot plume. A guess at the amount of permeability reduction may be made by considering simply the effect of fragmentation, a change from cracks say 5 cm apart (Table 1) to 0.4 mm apart (Coleman & Keith 1971). Equation (37) suggests that the permeability may change by a factor of  $10^4$  even without a porosity change in the shattered regions. In other zones where the cracked matrix is merely subjected to lateral rock-fabric pressure, the cracks would have to thin by a factor of 21 to cause a similar reduction in permeability (34), and the cross-bracing of the matrix is probably low enough to permit this. Thus, the permeability of the crushed region is likely to fall so much that essentially no flow will continue through it, and the hot plume will move or spread into surrounding rock. This situation is sketched in Fig. 6, where a hot plume has been presumed to spread around the collapsed region. The rock above and below the collapse will have some relief from overburden stress (regions h), and this stress will be added to regions j. They are now heated to the hot water temperature and under high stress; because of the upwelling blockage, the hot water temperature

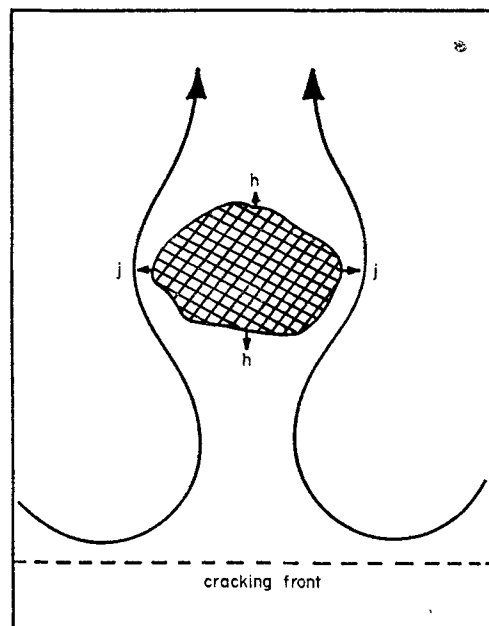


FIG. 6. Sketch of a hypothetical failed zone in a hot column, indicating possible propagation directions under concentrated stress and changing temperature.

will rise, and the failure will tend to propagate laterally as well as vertically at an accelerating rate.

As soon as the failed region has attained a significant lateral extent, cold water will leak into the high-permeability matrix above it and cool that rock to temperatures much lower than the original hot plume temperature. Upward growth of the collapsed zone will therefore be arrested, while lack of cold water access to the region underneath will accelerate failure by causing a general temperature increase. The final result is readily envisaged: the entire layer between the level of initial collapse and the cracking front will become relatively impermeable, while the region above it, insulated from the source of heat, will cool to near oceanic temperatures, and be frozen into a stable, high-permeability state. The cracking front may still advance slowly: the new regime in the collapsed layer is analogous to the original problem, in that it has a cool upper boundary and hot rock below. The permeability affecting the rate of heat transport is now independent of that near the cracking front, since the crushed layer is the principal barrier.

There are two quite divergent cases, depending upon whether the permeability in the crushed zone is or is not a strong function of temperature like that in the uncrushed matrix. If it is, as is most likely, a reasonable approximate formula for the front velocity may be obtained by combining equations (37) and (44):

$$u \simeq \frac{2\sqrt{2} y^2 \alpha^3 \alpha_w g (T - T_w)^3 (8T_w + T - 9T_0)}{12 \times 3240 v_w (T_1 - T_w)}. \quad (68)$$

For a typical cracking temperature of 800 °K,  $T_w$  maximizes  $u$  when it is 461 °K, and if the effective  $y$  is 0.04 cm, the front velocity is now

$$u \simeq 1.3 \times 10^{-8} \text{ cm s}^{-1} = 0.4 \text{ cm/yr}$$

$$D \simeq 2.5 \times 10^{-11} \text{ cm}^2 \quad (69)$$

Alternatively, if the permeability is no longer a function of temperature, and is fixed, say at  $2.5 \times 10^{-11} \text{ cm}^2$ , we can use equation (44) directly, choosing a reasonable water temperature, less than the cracking temperature, of 700 °K:

$$u \simeq 3.4 \times 10^{-7} \text{ cm s}^{-1} = 11 \text{ cm/yr}. \quad (70)$$

It should be noted that these are upper estimates, based on the assumption of an unchanged cracking temperature of 800 °K: the case in (69) implies a cracking temperature of more like 650 °K in Table 2 and a still slower rate of front advance. The significance of the results is that, following the formation of the collapsed layer, the rate of front advance drops by at least  $2\frac{1}{2}$  orders of magnitude and more probably four.

Hydrothermal penetration has not been stopped completely by the mechanical failure, and indeed it cannot be, but the rate of advance is now comparable to or slower than the rates of sea-floor spreading, and the normal processes of geological metamorphism have time to act. In fact, the crushed rock is prepared for the most rapid possible alteration, especially in the zones of total failure where the particle size is submillimetre. The hydrothermal temperatures of less than 700 °K are within the field of stability of most serpentinization products (Page 1967) and it is most likely that the temperature everywhere lies within the stability field of brucite, whose boundary is at 640 °K. Serpentinization of this type is essentially a constant composition process, notwithstanding the removal of small quantities of water-soluble ions in the hydrothermal brine (Corliss 1971), and involves a substantial volume expansion (Coleman & Keith 1971). Thus the metamorphic process is well capable

of finally sealing off all the porosity in the rock and terminating any deeper hydrothermal penetration.

The one-dimensional model generates a structure consisting of an upper layer of cold cracked rock open to water percolation and very slow metamorphism, a layer of mechanically crushed and rapidly metamorphosed impermeable rock, and the underlying mantle material now cooling slowly by conduction and no longer accessible to hydrospheric water. The cessation of penetration is a complex multistep process, requiring both static fatigue failure of the rock matrix and aqueous metamorphism in order to shut off the water access completely. The deeper mantle material may still crack if processes other than simple dislocation creep do not become important at the exceedingly slow distortion rates implied by large-scale conductive cooling, but now water has no ready access to these cracks. One may presume that volatile ( $\text{H}_2\text{O}$ ,  $\text{CO}_2$ ) induced grain recrystallization may be a fast enough aseismic process to accommodate the creep needed by the conductively cooling lithosphere.

#### 14. Discussion

If the one-dimensional model of water penetration so far derived has one salient characteristic, it is the rapid rate of advance of the cracking front. At 5 to 170 m/yr, the water can penetrate two to three orders of magnitude faster than seafloor can spread, provided it is given free enough access to the hot rock. The question is whether seawater ever does get such access at a (relatively) slow spreading ridge crest, or whether the model simply never applies because other phenomena dominate the spreading process. The problem is best discussed by reference to the structure of ophiolite suites, whose provenance as samples of the oceanic crust was suggested by Hess (1965) and is now fairly widely accepted (*cf.* Coleman 1971).

Underneath a variable thickness of pillow lavas, that must be extruded in direct contact with seawater, lies a 'sheeted complex' of 90–100 per cent dikes (Vine & Moores 1972). These dikes consist of basalt subjected to varying levels of greenschist metamorphism, a process that requires access by water. The very existence of a sheeted complex of significant (1 km) vertical extent *requires* water percolation cooling. If cooling of a spreading slab were by conduction to the top surface only, the lateral temperature gradient near the base of the layer would be far too low to result in recognizable dikes. The simplest order-of-magnitude calculation demonstrates this: the thermal time constant ( $h^2/2\kappa$ ) of 1 km of basalt is about 15 000 years, so that the time for half-cooling corresponds to a spreading of nearly  $\frac{1}{2}$  km at 3 cm/yr. In the field, the dikes show well-defined cooling edges and are of the order of 60 cm wide before being split by successive intrusion in the spreading process.

The level of initial permeability in the constructed sheeted complex depends on the ability of hydrothermal convection to keep the previously cracked material cool enough to prevent static fatigue failure and rapid metamorphism. Permeable convection near a hot vertical boundary has not been studied, but there is good reason to suppose that the vertical flow is broken into many small eddy-like cells. These can spread the heat laterally during the short time the dike must be emplaced in before the magma congeals. If this is the case, and the circumstantial evidence certainly suggests so, the cooling dike will crack across its width in much the same manner as a planar layer cracks three dimensionally. The presence of a 'skin' of material chilled without cracking reduces the overall shrinkage somewhat, and the presence of only one set of sub-parallel vertical cracks perpendicular to the dike plane reduces the vertical permeability by a factor of two. (Horizontal cracks could appear temporarily in the newest dikes, but cannot be maintained over any significant lateral distance as the structure so derived could hardly support the overburden pressure.) Before the eventual greenschist metamorphism sets in, the permeability of the sheeted

complex, and the pillow lavas above it, is more likely to be similar to that of the one-dimensional propagating model than of the collapsed layer discussed in the last section (equation (69)).

If water obtained access to the gabbroic material below the sheeted complex, it would be capable of propagating a cracking front downward with the velocities outlined in Table 1. Even brief thought about the mechanism of magma injection at the base of the sheeted complex suggests that this does not occur, at least not at the centre of accretion. A dike is formed when magma finds its way up through relatively cool country rock; if the region of dikes has a base, then the magma below that base has not been emplaced in such cool surroundings. Qualitatively, one can imagine an equilibrium spreading situation where the height of the immediately water-penetrated zone is established by the maximum permissible height of a dike emplaced into an effectively cooled medium, set by the fluidity, latent heat and supply pressure of the magma. The details of what happens at the base of the dike zone are not only obscure but rather important, since it is there that the symmetry or asymmetry of the spreading is decided. That zone also generates a layer that is impermeable to water, at least initially, and its thickness, temperature and strain history define the conditions under which further water penetration may occur. If there were no tectonic activity after construction of the sheeted complex, nothing more would happen except for the slow lithospheric cooling by conduction that causes the large scale mid-ocean ridge topography. Tectonic movement does continue to occur, however, as demonstrated by the existence of a central valley on many mid-ocean ridges, and the associated block tilting (Atwater & Mudie 1968). Both these features can be produced only by the emplacement of material from below *after* the formation of a crustal skin (Deffeyes 1970). The faulting associated with the block tilting would permit water access from the upper permeable layer into the relatively hot and uncracked material below. An experiment reported by Elder (1965) suggests that localized sources and sinks in the convection cell have very little effect on the hot-boundary flow and the rate of heat transfer from it. It is possible, therefore, that the one-dimensional model may apply qualitatively to what happens after faulting permits water access to the gabbroic layer: that penetration is rapid on a roughly planar front and is limited in depth by static fatigue, perhaps enhanced by a mineral assemblage change.

There is some circumstantial evidence that water penetration continues down to a depth comparable to that of the Mohorovicic discontinuity and it is this that makes the one-dimensional model worth discussing. The ultramafic rocks below the gabbroic layer in the ophiolite suites are substantially serpentinized (*cf.* Vine & Moores 1972), and although some of this could be associated with the uplift of the ophiolites, it is not obvious how large amounts of water could obtain access to bulk rock during large-scale tectonic events, for the fault zones are far apart. It is equally obscure how water access through deep cracks could cause 70 per cent serpentinization of such a rock, since there is a substantial expansion associated with the process that should close the cracks long before such a level of serpentinization is reached. From a cracking temperature of 800 °K, cooling to oceanic temperature would produce a rock volume contraction of about 1.5 per cent for predominantly vertical cracks. The volume expansion associated with in-place serpentinization of forsterite without removal of brucite ( $\text{Mg}(\text{OH})_2$ ) is about 50 per cent, using density data from Clark (1966). If present in the original rock, some calcium may be removed in solution by the hydrothermal waters, but even for original Hartzburgite (the basal layer of some ophiolite suites) the expansion is about 45 per cent. It is most unlikely that magnesium is effectively removed in hydrothermal systems (Page 1967) so that the maximum proportion of serpentinized material permitted by simple crack-filling is about 5 per cent, by volume. It is hard to see how the metamorphism could be irregular enough to permit a large expansion in an assemblage of sub-vertical macrocracks, but it may

be possible in the region shattered by static fatigue, where the initial fragment size is comparable to the size of the new mineral grains. Thus a relatively unexpected consequence of the one-dimensional penetration model could account for an otherwise rather awkward piece of field evidence, both as to the large proportion of serpentinization and its microstructure (Coleman & Keith 1971, previous discussion in static fatigue section).

Further circumstantial evidence that water penetrates deeper than the 1–2 km of the sheeted complex is provided by the ridge-crest heat-flow measurements. Values higher than 20 HFU ( $\mu \text{ cal cm}^{-2} \text{ s}^{-1}$ ) are absent, and the means for any one area are less than 6 HFU even when sedimentation is sufficient to permit a truly random distribution of the stations (Lister & Davis 1973). Now, if convection in a thin layer continues the normal crustal cooling by conduction below an impermeable boundary, the rate of heat transport through the convective layer is nearly the same as the surface heat flow of a purely conductive system. As soon as a relatively impermeable sediment covers the permeable layer (Lister 1972) the measured heat-flow should reflect approximately the conductive model values, so that if this occurs near the ridge crest, those values should be high. There is some evidence that this may happen well away from a ridge crest (Lister 1972), but never in a region that should produce a heat-flow of more than 10 HFU. Thus penetration *below the shut-off depth* should be sufficient to reduce the thermal flux through the remaining permeable zone to about 10 HFU or less, requiring about 3 km below that depth. This is consistent with a ridge crest where episodic one-dimensional water penetration occurs, but not with one where a stable impermeable boundary is maintained. It is also consistent with the measurement of high mantle seismic velocities near a ridge-crest (Bishop & Lewis 1973) at roughly normal intercept times (layer depth).

The detailed interpretation of marine seismic refraction results relative to the water penetration theory is difficult and can only be attempted in outline here. There are several curious features about the results that lend some support to the theory, but only in a highly circumstantial manner. One oddity is how remarkably consistent the depth to Moho seems to remain in spite of widely differing spreading rates where the crust was generated, and considerable variation in the crustal velocities, implying compositional differences (Raitt 1963). The difficulty of imagining how the right amount of basaltic differentiate should always be available helped to lead Hess (1959) to the conclusion that some physical phenomenon must determine the Moho depth, in his case the circa 500 °C serpentinization isotherm. It would be attractive indeed if the consistency of Moho depth could be attributed to the existence of a partially serpentinized ultramafic layer, even though the water penetration model lacks something in elegance and simplicity. The principal objection to the idea has always been the consistency of layer 3 velocities at a value ( $6.7 \text{ km s}^{-1}$ ) implying an awkwardly high degree of arbitrary serpentinization. However, the existence of a well-defined gabbroic layer 3 (ophiolites: Vine & Moore 1972; acoustic velocities: Christensen 1969) does not preclude the presence of a higher velocity partially serpentinized layer above the Moho. Sutton, Maynard & Hussong (1971) describe repetitive source refraction evidence for just such a layer, and cite occurrences of detectable layer 4 s in prior refraction work. It is interesting that their mean basal layer velocity is about  $7.4 \text{ km s}^{-1}$ , and would correspond, on a summed compressibility model, to about 15 per cent by volume serpentine remainder dunite. This is three times the amount of serpentine that could be replaced by simple crack filling after cracking at 800 °K and cooling, but the calculation has taken no account of the velocity anisotropy expected of a structure containing vertical veins of serpentine. Moreover, even the refined acoustic technique of the above authors would be unable to detect a still higher velocity layer just above Moho, and they may simply be observing the boundary between the gabbros and the uppermost layer of serpentinized ultramafic material. Finally, further circumstantial evidence that low grade metamorphism may be taking

place deep in young oceanic crust is the apparent increase in thickness of layer 3 with distance from the ridge crest (Le Pichon 1969). This is more likely to be due to a decrease in the seismic velocity of material above the impermeable collapse zone than to an actual deepening of the water penetration, but it cannot be explained by non-metamorphic mineral rearrangements, either in gabbroic material, or in the ultramafic layer beneath.

## 15. Conclusions

The circumstantial evidence that water penetrates to a substantial depth in young oceanic crust is strong but not specific. Ridge crest heat-flow values, surface sediment composition and seismic refraction results are all inconsistent with a plate spreading model limited to conductive cooling through the surface. Inconsistent also, though less conclusively perhaps, are the sheeted dike complexes of ophiolite suites and the magnetic anomaly layer accurately recording geomagnetic reversals (Heirtzler *et al.* 1968), though the latter is probably the best evidence that the former is widespread in the oceanic crust. Further interpretation of these vague inconsistencies and odd results requires some understanding of the physical process that seems to be responsible: the penetration of water into hot rock. This paper has made a sub-first-order attempt to delineate the applicable physics by considering a highly oversimplified model, and deriving its expected behaviour. The results are quite startling and seem to be consistent with most of the observational data.

In summary, water is readily able to penetrate downward into hot rock by convection in a propagating matrix of cracks. The rate of advance of the cracking 'front' is high, of the order of 30 m/yr, and is only a weak function of depth. A rudimentary treatment of the theory of transient creep, fitted to probably inaccurate data, suggests that cracking should occur between 800 and 1000 °K, and that the cracking temperature also should be a weak function of overburden pressure. The depth of penetration is not limited directly by any phenomenon associated with the opening of the cracks, at least not at reasonable crustal depths of about 7 km or less. Rather, the limiting phenomenon appears to be static fatigue of the polygonal columns isolated by the cracks, under the influence of the differential overburden pressure, the moderately elevated temperature (~460 °K) and possibly the weakening effect of water. Lifetimes between 0.1 and 100 000 years are plausible on the basis of limited data and rudimentary theory, while an order of magnitude of 100 years would fit best to the circumstantial evidence (heat-flow and topography). The phenomenon of static fatigue itself provides a ready rationale for volume distributions of microearthquakes and could be used as an explanation for the curious structure of partially serpentinized rocks. Finally, if the ophiolite suite structure of a sheeted dike complex overlying low-grade metamorphosed gabbroic and ultramafic rocks is representative of the oceanic crust, the one-dimensional model may even apply to episodic water penetration below the sheeted complex itself.

The question that remains is whether the water penetration theory, thus far developed, is capable of making any useful predictions. The gross geophysical mechanism of crust formation appears to be so messy that clear and simple predictions are not likely by *any* theory. About all that can be said is that the episodic rapid penetration of water to Moho depths is likely to be associated with the phenomenon of central valley formation, for without it magma should always be able to penetrate to the surface by dike formation and the transition to block uplift should not occur. The probable association of block faulting with the access of water to the deeper layers of hot rock leads to the possibility of a bi-stable condition: if a central valley is formed, it immediately becomes a prominent and stable feature. What happens at a fast-spreading ridge is still obscure, since it is there that high seismic velocities have been measured *across* the crest at mantle depths (Bishop & Lewis 1973). As regards



phenomena of a smaller scale, the existence of episodic one-dimensional penetration, followed by static fatigue, suggests that there should be volumetrically localized microearthquake swarms at relatively isolated places along the ridge crest. These earthquakes should be distinguishable from the more usual shear-faulting type by the lack of polarity changes of the first motions in the azimuthal plane.

It is in the realm of hydrothermal conditions that the theory can make reasonably clear predictions. The permeability of the rock matrix should be high—over  $10^{-7}$  cm<sup>2</sup>—and consequently hydrothermal temperatures should be low ( $\sim 460$  °K). The usual condition at the ridge crest is moderate hydrothermal activity in the sheeted-complex-magnetic layer, extracting heat conducted from below and from a central dike emplaced every 3 to 30 years. In the rare places where episodic deeper penetration occurs, hydrothermal activity should be vigorous and involve very high thermal powers per unit area: up to  $15$  kW m<sup>-2</sup>. Over a spent penetration area, where static fatigue collapse near the top of the ultramafic layer is nearly complete, the upper crust should be essentially cold, with an even higher permeability than normal. For there the heat source below will have been cut off, and it takes about 130 000 years for a conductive gradient to be re-established in a layer 2 km thick (for example). These areas should be those where the measured surficial heat-flow is unusually low.

I hope this theoretical presentation will serve to stimulate some experimental work on both rock mechanical properties and appropriate sampling for interstitial waters during oceanic hard-rock drilling. Even if the predictions made here turn out to be wrong, something useful will have been learned. If, indeed, hydrothermal penetration is as pervasive and vigorous as the calculations suggest, the mid-ocean ridge crests could turn out to be significant sources of both power and minerals in spite of the high costs of underwater drilling and power engineering. The costs of researching the matter are small compared to those involved in the development of fusion reactors, and there is little doubt that the geothermal power is *there* in some form or another. Artificial stimulation of power production from regions of uncracked hot rock also seems to be a good possibility, and such a technique would not be limited to oceanic ridge crests.

### Acknowledgments

This work was supported by grants GA-27947 and GA-38351 from the National Science Foundation of the USA. I particularly thank Dr A. H. Lachenbruch for his help with comments and reprints that set the discussion of cracking onto the right track. I also wish to thank Dr Bernard Evans for supplying excellent background material on ultramafic rocks, without which a non-geologist would have been completely confused.

*Geophysics Group and Department of Oceanography,  
University of Washington, WB-10,  
Seattle, Washington 98195, USA.*

### References

- Atwater, T. M. & Mudie, J. D., 1968. Block faulting on the Gorda Rise, *Science*, **159**, 729.
- Beard, C. N., 1960. Quantitative study of columnar jointing, *Geol. Soc. Am. Bull.*, **70**, 379.
- Bender, M., Dymond, J. R. & Heath, G. R., 1971. Isotopic analyses of metalliferous sediments from the East Pacific Rise, *Geol. Soc. Am. Abstr.*, **3**, 537.

- Bishop, T. N. & Lewis, B. T. R., 1973. Seismic refraction results from the East Pacific Rise near 14° N 104° W, *EOS*, **54**, 377 (abstract).
- Bodvarsson, G. & Lowell, R. P., 1972. Ocean-floor heat-flow and the circulation of interstitial waters, *J. geophys. Res.*, **77**, 4472.
- Booker, J. R., 1972. Large amplitude convection with strongly temperature variable viscosity, *Trans. Am. geophys. Un.* (abstract), **53**, 520.
- Bostrom, K. & Peterson, M. N. A., 1969. The origin of aluminium ferro-manganous sediments in areas of high heat-flow on the East Pacific Rise, *Mar. Geol.*, **7**, 427.
- Carslaw, H. S. & Jaeger, J. C., 1959. *Conduction of heat in solids*, 2nd edition, Oxford University Press.
- Carter, N. J. & Ave'Lallement, H. G., 1970. High temperature flow of dunite and peridotite, *Geol. Soc. Am. Bull.*, **81**, 2181.
- Christensen, N. I., 1969. Composition and evolution of the oceanic crust, *Mar. Geol.*, **8**, 139.
- Clark, S. P., Editor, 1966. Handbook of physical constants, *Geol. Soc. Am. Mem.*, **97**.
- Coleman, R. G., 1971. Plate tectonic emplacement of upper mantle peridotites along continental edges, *J. geophys. Res.*, **76**, 1212.
- Coleman, R. G. & Keith, T. E., 1971. A chemical study of serpentinisation—Burro Mountain, California, *J. Petrol.*, **12**, 311.
- Corliss, J. B., 1971. The origin of metal-bearing submarine hydrothermal solutions, *J. geophys. Res.*, **76**, 8128.
- Corte, A. & Higashi, A., 1960. Experimental research on desiccation cracks in soil, *SIPRE Rept.*, **66**.
- Deffeyes, K. S., 1970. The axial valley: A steady state feature of the terrain, in *Megatectonics of continents and oceans*, ed. H. Johnson, Rutgers University Press, New Brunswick, N.J.
- Elder, J. W., 1965. Physical processes in geothermal areas, *Am. geophys. Un. Mono.*, **8**, 211.
- Green, H. W. & Radcliffe, S. V., 1972. Dislocation mechanisms in olivine and flow in the upper mantle, *Earth Planet Sci. Letters*, **15**, 239.
- Harlow, F. H. & Pracht, W. E., 1972. A theoretical study of geothermal energy extraction, *J. geophys. Res.*, **77**, 7038.
- Heirtzler, J. R., Dickson, G. O., Herron, E. M., Pitman, W. C. & Le Pichon, X., 1968. Marine magnetic anomalies, geomagnetic field reversals and motions of the ocean floor and continents, *J. geophys. Res.*, **73**, 2119.
- Hess, H. H., 1959. The AMSOC hole to the Earth's mantle, *Trans. Am. geophys. Un.*, **40**, 340.
- Hess, H. H., 1962. History of ocean basins, in *Petrologic Studies* (Buddington Vol.), eds. A. E. J. Engel, H. L. James, & B. F. Leonard, *Geol. Soc. Am.*, 599.
- Hess, H. H., 1965. Mid-ocean ridges and tectonics of the sea floor, *Colston Papers*, Proc. 17th Symp. Colston Research Soc., Univ. Bristol, Butterworths Sci. Pub., 317.
- Hillig, W. B. & Charles, R. J., 1965. Surfaces, stress dependent surface reactions, and strength, in *High Strength Materials*, ed. V. Zackay, pp. 682–705, John Wiley, New York.
- Irwin, G. R., 1958. Fracture, in *Handbuch der Physik*, ed. S. Flugge, pp. 551–590, Springer, Berlin, Vol. 6.
- Kats, A., 1962. Hydrogen in alpha-quartz, *Phillips Res. Repts.*, **17**, 133.
- Lachenbruch, A. H., 1961. Depth and spacing of tension cracks, *J. geophys. Res.*, **66**, 4273.
- Lachenbruch, A. H., 1962. Mechanics of thermal contraction cracks and ice-wedge polygons in permafrost, *Geol. Soc. Am. Spec. Paper*, **70**.
- Lapwood, E. R., 1948. Convection of a fluid in a porous medium, *Proc. Camb. phil. Soc.*, **44**, 508.

- Le Pichon, X., 1969. Models and structure of the oceanic crust, *Tectonophysics*, **7**, 385.
- Lister, C. R. B., 1972. On the thermal balance of a mid-ocean ridge, *Geophys. J. R. astr. Soc.*, **26**, 515.
- Lister, C. R. B. & Davis, E. E., 1973. Heat-flow variations across the Sovanco fracture zone, *EOS*, **54**, 462 (abstract).
- Martin, R. J., 1972. Time-dependent crack growth in quartz and its application to the creep of rocks, *J. geophys. Res.*, **77**, 1406.
- Muskhelishvili, N. I., 1953. *Some basic problems of the mathematical theory of elasticity*, P. Noordhoff, Groningen, The Netherlands, 704 pp.
- Nur, A. & Booker, J. R., 1972. Aftershocks caused by pore fluid flow?, *Science*, **175**, 885.
- Page, N. J., 1967. Serpentinisation considered as a constant volume metasomatic process: a discussion, *Am. Mineralogist*, **52**, 545.
- Palmason, G., 1967. On heat-flow in Iceland in relation to the Mid-Atlantic Ridge, in *Iceland and Mid-Ocean Ridges*, Publ. **38**, ed. S. Bjornsson, pp. 111–127, Soc. Sci. Islandica, Reykjavik.
- Piper, D. Z., 1973. Origin of metalliferous sediments from the East Pacific Rise, *Earth Planet. Sci. Lett.*, **19**, 75.
- Raitt, R. W., 1963. The crustal rocks, in *The Sea*, 3, edited by M. N. Hill, Interscience, New York, 85.
- Ree, F. H., Ree, T. & Eyring, H., 1960. Relaxation theory of creep of metals, *Am. Soc. Civ. Eng., Eng. Mech. Div. J.*, **86**, 41.
- Scholtz, C. H., 1972. Static fatigue of quartz, *J. geophys. Res.*, **77**, 2104.
- Sutton, G. H., Maynard, G. L. & Hussong, D. M., 1971. Widespread occurrence of a high velocity basal layer in the Pacific crust found with repetitive sources and sonobuoys, in The structure and physical properties of the Earth's crust, Geophysical Monograph, **14**, *Am. Geophys. Un.*, 193.
- Talwani, M., Windisch, C. C. & Langseth, M. G., 1971. Reykjanes ridge crest: a detailed geophysical study, *J. geophys. Res.*, **76**, 473.
- Timoshenko, S. P. & Goodier, J. N., 1970. *Theory of Elasticity*, 3rd Ed., McGraw-Hill, N.Y.
- Vine, F. J. & Moores, E. M., 1972. A model for the gross structure, petrology and magnetic properties of oceanic crust, *Geol. Soc. Am. Mem.*, **132**, 195.
- Ward, P. L., 1972. Microearthquakes: prospecting tool and possible hazard in the development of geothermal resources, *Geothermics*, **1**, 3–12.
- Weertman, J., 1970. The creep strength of the Earth's mantle, *Rev. Geophys. Space Phys.*, **8**, 145.
- Wilden, R. & Mabey, D. R., 1961. Giant dessication fissures on the Black Rock and Smoke Creek deserts, Nevada, *Science*, **133**, 1359.

## Appendix I

### List of Symbols

Greek symbols follow nearest equivalent Latin letter.

$\mathcal{A}$  = Rayleigh stability number for percolation convection,

$\mathcal{A}_c$  = critical Rayleigh number,

$\alpha$  = coefficient of linear expansion of rock  $\sim 1.5 \times 10^{-5} \text{ }^\circ\text{K}^{-1}$  (Clark 1966),

$\alpha_w$  = coefficient of cubical expansion of water  $\sim 4.2 \times 10^{-6}$  ( $T - 273$ ), for  $370 < T < 570 \text{ }^\circ\text{K}$  (Elder 1965),

- $c$  = specific heat of rock  $\sim 0.24 \text{ cal g}^{-1} \text{ }^\circ\text{K}^{-1}$ ,  
 $C_{\text{H}_2\text{O}}$  = water concentration, molar,  
 $\gamma$  = water concentration exponent, Scholtz (1972) formula,  
 $d$  = crack width (cm),  
 $D$  = permeability ( $\text{cm}^2$ ),  
 $E$  = creep constant ( $\text{s}^{-1}$ ),  
 $\varepsilon$  = equivalent vertical strain, compression positive,  
 $\dot{\varepsilon}$  = rate of plastic strain, equivalent vertical, compression positive,  
 $\dot{\varepsilon}_H$  = rate of horizontal plastic strain, compression positive,  
 $\varepsilon_\phi$  = creep after cracking, equivalent uniaxial,  
 $\dot{\varepsilon}_\phi$  = rate of creep at overburden pressure just prior to cracking, equivalent uniaxial,  
 $f(\sigma, T)$  = generalized stress dependence of creep,  
 $F$  = diffusion rate for moisture ( $\text{cm}^2 \text{ s}^{-1}$ ),  
 $F_0$  = reference moisture diffusion rate  $\sim 5.5 \times 10^{-5} \text{ cm}^2 \text{ s}^{-1}$  (Kats 1962),  
 $g$  = acceleration of gravity, cgs,  
 $h$  = depth of convecting slab (cm),  
 $H$  = molar activation energy for creep, kcal/mole,  
 $H'$  = molar activation energy for static fatigue, kcal/mole  $\sim 24$  (Scholtz 1972),  
 $H''$  = molar activation energy for moisture diffusion, kcal/mole  $\sim 19.3$  (Kats 1962),  
 $\eta$  = viscosity of percolating fluid,  
 $\theta$  = ratio of crack spacing to thermal boundary layer thickness,  
 $k$  = crack edge stress intensity factor,  $\text{kb cm}^{\frac{1}{2}}$ ,  
 $\kappa$  = diffusivity of rock  $\sim 0.009 \text{ cm}^2 \text{ s}^{-1}$ ,  
 $\kappa'$  = effective diffusivity of porous medium for Rayleigh number calculation  $\sim \kappa$ ,  
 $\xi$  = new variable of integration,  
 $m$  = creep law exponent for stress,  
 $M$  = planar modulus =  $Y(1-n)^{-1}$ ,  
 $n$  = Poisson's ratio for rock = 0.35 (Clark 1966),  
 $\mathcal{N}$  = Nusselt number,  
 $\nu_w$  = kinematic viscosity of water  $\sim 0.33 (T-273)^{-1}$  stokes,  
 $370 < T < 470 \text{ }^\circ\text{K}$  (Elder 1965),  
 $\Omega$  = molar activation volume for creep kcal/kb,  
 $\Omega'$  = molar activation volume for fatigue, kcal/kb,  
 $P$  = total water pressure (bars),  
 $P_i$  = water pressure in the central region of a rock column,  
 $P_0$  = water pressure outside a rock column,  
 $\mathcal{P}$  = overburden pressure (kb),  
 $\phi$  = correction factor between cracking of quartz and of mafic rock in polygonal system,  
 $Q$  = heat transport per unit area,  
 $R$  = gas constant =  $0.002 \text{ kcal mole}^{-1} \text{ }^\circ\text{C}^{-1}$ ,

- $\rho$  = density of rock =  $3.2 \text{ g cm}^{-3}$  (Clark 1966),  
 $s$  = instantaneous weakening rate of rock under stress,  
 $\sigma$  = equivalent vertical stress (kb),  
 $\sigma_c$  = excess vertical compressive stress equivalent to cracking tension =  $\sigma - \mathcal{P}$ ,  
 $\sigma_H$  = equivalent horizontal stress due to overburden,  
 $\sigma_m$  = crack propagating stress for Martin (1972) experimental geometry and quartz,  
 $\sigma_0$  = activation stress for creep (kb),  
 $\sigma_0'$  = activation stress for fatigue =  $0.8 \text{ kb}$  (Scholtz 1972),  
 $\sigma_1$  = stress at 1 per cent uniaxial strain (kb),  
 $t$  = time, s or yr,  
 $t_0$  = reference fatigue life =  $2 \times 10^5 \text{ s}$  at  $300^\circ\text{K}$ , 1 b water, 15 kb (Scholtz 1972),  
 $\langle t \rangle$  = static fatigue life, statistical mean,  
 $T$  = temperature,  $^\circ\text{K}$ ,  
 $T_K$  = cracking temperature,  
 $T_{\mathcal{P}}$  = temperature at which overburden pressure is supported by creep stress,  
 $T_W$  = water temperature near the hot boundary,  
 $T_0$  = reservoir temperature (ocean) =  $275^\circ\text{K}$ ,  
 $T_1$  = initial rock temperature =  $1500 \pm 50^\circ\text{K}$  (magma eruption, Clark 1966),  
 $T_2$  = hot boundary effective temperature,  
 $\Delta T$  = temperature difference across convecting slab,  
 $\Delta T_r$  = radial temperature difference in a column,  
 $\tau$  = time to half permeability,  
 $u$  = cracking front velocity ( $\text{cm s}^{-1}$  or  $\text{m/yr}$ )  
 $v$  = water flow velocity,  
 $x$  = distance measured below cracking front,  
 $x_0$  = boundary layer thickness ( $1/e$ ), (cm or m),  
 $y$  = crack spacing, mean (cm),  
 $Y$  = Young's modulus for rock =  $1.5 \text{ Mb}$  (Clark 1966).